1   Total organic carbon and contribution from speciated organics in cloud water: Airborne data
2   analysis from the CAMP²Ex field campaign

3   Connor Stahl[1], Ewan Crosbie[2,3], Paola Angela Bañaga[4,5], Grace Betito[4], Rachel A. Braun[1], Zenn
4   Marie Cainglet[4,5], Maria Obiminda Cambaliza[4,5], Melliza Templonuevo Cruz[4,6], Julie Mae
5   Dado[7], Miguel Ricardo A. Hilario[4,8], Gabrielle Frances Leung[4,9], Alexander B. MacDonald[1],
6   Angela Monina Magnaye[7], Jeffrey Reid[10], Claire Robinson[2,3], Michael A. Shook[2], James
7   Bernard Simpas[4,5], Shane Marie Visaga[5,7], Edward Winstead[2,3], Luke Ziemba[2], Armin
8   Sorooshian[1,8]

9   [1]Department of Chemical and Environmental Engineering, University of Arizona, Tucson,
10   Arizona, 85721, USA

11   [2]NASA Langley Research Center, Hampton, Virginia, 23666, USA

12   [3]Science Systems and Applications, Inc., Hampton, Virginia, 23666, USA

13   [4]Air Quality Dynamics-Instrumentation & Technology Development Laboratory, Manila
14   Observatory, Quezon City, 1108, Philippines

15   [5]Department of Physics, School of Science and Engineering, Ateneo de Manila University,
16   Quezon City, 1108, Philippines

17   [6]Institute of Environmental Science and Meteorology, University of the Philippines, Diliman,
18   Quezon City, 1101, Philippines

19   [7]Regional Climate Systems Laboratory, Manila Observatory, Quezon City, 1108, Philippines

20   [8]Department of Hydrology and Atmospheric Sciences, University of Arizona, Tucson, Arizona,
21   85721, USA

22   [9]Department of Atmospheric Science, Colorado State University, Fort Collins, Colorado 80521,
23   USA

24   [10]Marine Meteorology Division, Naval Research Laboratory, Monterey, California 93943, USA

25   *Correspondence to: armin@email.arizona.edu*

26   **Abstract**

27   This work focuses on total organic carbon (TOC) and contributing species in cloud water over
28   Southeast Asia using a rare airborne dataset collected during NASA's Cloud, Aerosol and
29   Monsoon Processes Philippines Experiment (CAMP^{2}Ex), in which a wide variety of maritime
30   clouds were studied, including cumulus congestus, altocumulus, altostratus, and cumulus.
31   Knowledge of TOC masses and their contributing species is needed for improved modeling of
32   cloud processing of organics and to understand how aerosols and gases impact and are impacted
33   by clouds. This work relies on 159 samples collected with an Axial Cyclone Cloud water
34   Collector at altitudes of 0.2 – 6.8 km that had sufficient volume for both TOC and speciated
35   organic composition analysis. Species included monocarboxylic acids (glycolate, acetate,
36   formate, and pyruvate), dicarboxylic acids (glutarate, adipate, succinate, maleate, and oxalate),
37   methanesulfonate (MSA), and dimethylamine (DMA). TOC values range between 0.018 – 13.66
38   ppm C with a mean of 0.902 ppm C. The highest TOC values are observed below 2 km with a
39   general reduction aloft. An exception is samples impacted by biomass burning for which TOC
40   remains enhanced as high as 6.5 km (7.048 ppm C). Estimated total organic matter derived from
41   TOC contributes a mean of 30.7% to total measured mass (inorganics + organics). Speciated
42   organics contribute (on carbon mass basis) an average of 30.0% to TOC in the study region, and
43   account for an average of 10.3% to total measured mass.

44   The order of the average contribution of species to TOC, in decreasing contribution of carbon
45   mass, is as follows (± one standard deviation): acetate (14.7 ± 20.5%), formate (5.4 ± 9.3%),
46   oxalate (2.8 ± 4.3%), DMA (1.7 ± 6.3%), succinate (1.6 ± 2.4%), pyruvate (1.3 ± 4.5%),
47   glycolate (1.3 ± 3.7%), adipate (1.0 ± 3.6%), MSA (0.1 ± 0.1%), glutarate (0.1 ± 0.2%), maleate
48   (< 0.1 ± 0.1%). Approximately 70% of TOC remains unaccounted for, thus highlighting the
49   complex nature of organics in the study region; samples collected in biomass burning plumes
50   have up to 95.6% of unaccounted TOC mass based on the species detected. Consistent with other
51   regions, monocarboxylic acids dominate the speciated organic mass (~75%) and are about four
52   times in greater abundance than dicarboxylic acids.

53   Samples are categorized into four cases based on back-trajectory history revealing source-
54   independent similarity between the bulk contributions of monocarboxylic and dicarboxylic acids
55   to TOC (16.03% – 23.66% and 3.70% – 8.75%, respectively). Furthermore, acetate, formate,
56   succinate, glutarate, pyruvate, oxalate, and MSA are especially enhanced during biomass burning
57   periods, attributed to peat emissions transported from Sumatra and Borneo. Lastly, dust (Ca^{2+})
58   and sea salt (Na$^+$/Cl$^-$) tracers exhibit strong correlations with speciated organics, thus supporting
59   how coarse aerosol surfaces interact with these water-soluble organics.

60

1. Introduction

The last two decades witnessed an acceleration of research to unravel the nature of the organic fraction of airborne particles, including speciation (Hallquist et al., 2009; Kanakidou et al., 2005), with implications for how particles impact air quality, public health, and the planet's energy balance. However, there has been much less progress on organic research for cloud droplets, owing largely to the inaccessibility of clouds as compared to particles that can be measured more easily near the surface. Analyzing organic matter in cloud water will lead to better understanding of secondary aerosol formation and the nature of cloud condensation nuclei (CCN) that form droplets. The interaction of aerosol particles and clouds interact constitutes the largest uncertainty in estimating total anthropogenic radiative forcing (IPCC, 2013), which motivates using cloud composition as a tool to learn about these processes (MacDonald et al., 2020). Characterizing cloud water composition is insightful for atmospheric chemical processes such as the removal of gases that would otherwise participate in gas-phase reactions and for aqueous reactions that yield products without an efficient gas-phase source (e.g., dicarboxylic acids) (Ervens et al., 2013). While modeling of sulfate production in clouds is fairly mature (Barth et al., 2000; Faloona, 2009; Kreidenweis et al., 2003; Liu et al., 2021), the formation and evolution of organics in cloud water is much more poorly constrained (Ervens, 2015).

Advancing this research requires in situ measurements of cloud water composition. Among the most common methods of characterizing the organic fraction of cloud water samples is total organic carbon (TOC) analysis. Whether it is cloud water or fog water, most studies have shown that (i) TOC is enhanced in air masses with higher anthropogenic influence (Collett Jr. et al., 1998; Deguillaume et al., 2014; Herckes et al., 2013; Raja et al., 2009); (ii) ~40% – 85% of the TOC is attributed to unidentified species (Benedict et al., 2012; Boris et al., 2016; Boris et al., 2018; Herckes et al., 2002; Raja et al., 2008); (iii) organic acids usually account for ≲15% of the TOC (Deguillaume et al., 2014; Gioda et al., 2011; Straub et al., 2007); (iv) monocarboxylic acids are more abundant than dicarboxylic acids (Löflund et al., 2002); and (v) acetic and formic acids are the most dominant organic acids contributing to TOC (Collett Jr. et al., 2008; Gioda et al., 2011). Most of the aforementioned studies focused on fog, therefore motivating a closer look at cloud water, as solute concentrations depend on the type of aqueous medium (Fig. 1). More specifically, TOC concentrations are reported to be higher in fog water relative to rain water (Kim et al., 2020), while cloud water solute concentrations exceed those in rain water (Decesari et al., 2005; Gioda et al., 2008).

Southeast Asia is an ideal laboratory to investigate the nature of TOC and its constituents as it is impacted by a multitude of emissions sources in an environment with persistent cloud cover from a variety of cloud types (e.g., shallow cumulus and cumulus congestus clouds) (Reid et al., 2013). The complex meteorology of the region makes it very difficult to model (Wang et al., 2013; Xian et al., 2013), but simultaneously provides a remarkable opportunity to learn more about how aerosols impact (and are impacted by) tropical cloud systems. A knowledge gap exists as there have been no studies of cloud composition in this region based on airborne measurements. Analysis of fog water at Baengnyeong Island in the eastern Yellow Sea revealed that organic acids accounted for 36 – 69% of TOC (Boris et al., 2016). The Acid Deposition

102 Monitoring Network in East Asia (https://www.eanet.asia/) provides data on wet deposition at
103 surface sites such as at the Manila Observatory (Metro Manila, Philippines) (Ma et al., 2021) and
104 is limited to inorganic ions. Previous studies such as the Seven South East Asian Studies
105 (7SEAS) (Reid et al., 2013) and the Cloud, Aerosol and Monsoon Processes Philippines
106 Experiment (CAMP²Ex) weatHEr and CompoSition Monitoring (CHECSM) were carried out in
107 this region; however, these campaigns were ground and ship-based, and focused mainly on
108 aerosol particles and not cloud composition (Hilario et al., 2020b; Reid et al., 2015; Reid et al.,
109 2016). It should also be noted that there have also been a handful of high elevation studies
110 carried out in Southeast Asia examining fog and cloud water organic acids (i.e., Decesari et al.,
111 2005; Li et al., 2017; Mochizuki et al., 2020).

112 Recent studies in Metro Manila, Philippines provide the following results of relevance to this
113 work: (i) a third to a half of the total aerosol particle mass is often unaccounted for after
114 considering water-soluble species (inorganic and organic acid ions and elements) and black
115 carbon (Cruz et al., 2019; Stahl et al., 2020); (ii) organic acids account for less than 1% of total
116 aerosol mass, with oxalate being the most abundant acid (Stahl et al., 2020); (iii) organic acid
117 concentrations are more enhanced during biomass burning periods (Hilario et al., 2020a),
118 especially succinate and oxalate (Braun et al., 2020; Stahl et al., 2020); and (iv) wet deposition
119 samples clearly show the influence of biomass burning tracer species on cloud composition (Ma
120 et al., 2021). Based on these points, we test two hypotheses: (i) the relative contribution of
121 organic acids to TOC will exceed what was observed at the surface layer over Metro Manila
122 owing to more aged air masses aloft as compared to the surface layer in Metro Manila exposed to
123 fresher emissions; and (ii) clouds impacted by biomass burning emissions will exhibit chemical
124 profiles shifted to higher TOC concentrations and with a greater portion of that TOC accounted
125 for by organic acids. To address these hypotheses in addition to characterizing the organic
126 fraction of cloud water, we utilized a rich set of cloud water samples collected around the
127 Philippines during CAMP²Ex between August and October in 2019. The subsequent results and
128 discussion focus on TOC concentrations in addition to the relative contribution and
129 interrelationships between a suite of organic species (organic acids, methanesulfonate,
130 dimethylamine) spatially, and as a function of altitude and air mass source origin. A unique
131 aspect of this dataset is the large sample number with both TOC and speciated organic acid
132 information from an airborne platform.

133

2. Methods
2.1 Study overview

136 A total of 159 cloud water samples were collected on the NASA P-3B Orion aircraft across 19
137 research flights (RF; 23 August – 5 October 2019) during CAMP²Ex that were measured for
138 ions, pH, and TOC. Flights were based out of Clark International Airport (15.189°N, 120.547°E)
139 and extended to regions around the island of Luzon (Fig. 2). Cloud water samples were collected
140 over a wide range of altitudes ranging from 0.2 – 6.8 km.

141

2.2 Cloud water collection and handling

Samples were collected using the Axial Cyclone Cloud water Collector (AC3), (Crosbie et al., 2018), which efficiently (> 60% collection efficiency) collects cloud droplets with diameters > 20 µm. The size dependence of the collection efficiency may influence the measured properties of the bulk cloud water in cases where there is a strong size-dependence in the droplet composition. Sample water evaporation was identified to affect low liquid water content environments and may increase aqueous concentrations. For this study the pipe position was set to position 10, as described in Crosbie et al. (2018), and mounted to the fuselage pylon approximately 300 mm from the skin. The AC3 has a shutter attached to a servo motor allowing the collector to be closed when not in a cloud to prevent contamination. Samples were collected between 10 seconds and 10 minutes depending on cloud availability and liquid water content (i.e., shorter times possible with higher liquid water content). Cloud water was collected in prewashed 15-mL plastic conical vials. Due to thorough prewashing of the plastic conical vials, leaching of organics into samples was negligible. Additional laboratory tests also indicated that there was no appreciable evidence that organics were adsorbing to the walls of the conical vials. Before each flight, the collector was flushed with ~ 1 L of ultra-purified Milli-Q water (18.2 MΩ-cm) prior to obtaining two blank samples. Blanks were also collected post-flight that were similarly flushed prior to being collected. During flight, samples were collected and stored in a cooler with sufficient ice packs to reduce possible decomposition. After flights, samples were immediately taken to an onsite laboratory where sample volumes were recorded and analyzed for ionic composition, TOC, and pH. A background was subtracted from the samples based on the bottom 10th percentile of all blanks collected during the campaign (both pre- and post-flight). The 10th percentile of the blanks was used instead of the mean as it is a compromise between removing the influence of background contamination and conserving data points. Excess samples were stored in a refrigerator for future analyses that are outside the scope of this study.

2.3 Cloud water analysis
2.3.1 Ion chromatography

Cloud water was speciated using ion chromatography (IC; Dionex ICS-2100) immediately after each flight to reduce the possibility of degradation of the samples. Measured anionic species of interest were glycolate, acetate, formate, methanesulfonate, pyruvate, glutarate, adipate, succinate, maleate, oxalate, Cl^-, NO_2^-, Br^-, NO_3^-, and SO_4^{2-}. Measured cations were Na^+, NH_4^+, K^+, dimethylamine (DMA), Mg^{2+}, and Ca^{2+}. A 23-minute instrument method was used for both anion and cation columns with a 2-minute equilibration period, yielding a 25-minute sampling period per sample. The instrument flow rate was 0.4 mL min^{-1}. The anions were measured using a Dionex IonPac AS11-HC 2 × 250 mm column, a Dionex AERS 500e suppressor, and with potassium hydroxide as the eluent. The cations were measured using a Dionex IonPac CS12A 2 × 250 mm column, a Dionex CERS 500e suppressor, and using methanesulfonic acid (MSA) as the eluent. The instrument methods used for analysis are as follows: (i) for anions the eluent concentration started at 1 mM, ramped up to 4 mM between 0 – 10 minutes, ramped up to 6 mM between 10 – 11 minutes, and finally ramped up to 7 mM between 11 – 23 minutes using a

183 suppressor current of 8 mA; (ii) for cations the eluent concentration started at 5 mM and
184 remained isocratic from 0 – 10 minutes, ramped up to 18 mM between 10 – 12 minutes, and
185 finally remained isocratic at 18 mM from 12 – 23 minutes using a suppressor current of 22 mA.
186 The limits of detection (LOD) for these species can be found in Table 1 and were calculated
187 using $3S_a b^{-1}$ where S_a is the standard deviation of the response and b is the slope of the
188 calibration curve for that species.

189

2.3.2 Total organic carbon and pH

191 Total organic carbon (TOC) was measured using a Sievers 800 Turbo TOC analyzer. Sample
192 aliquots were diluted to obtain the minimum volume needed by the instrument. The TOC
193 analyzer was operated in turbo mode and TOC values were averaged over a stable concentration
194 period. Milli-Q water was used as an internal reference and calibrations were performed before
195 and after each batch of samples was analyzed (i.e., one batch every ~3 – 4 flights) using a range
196 of different concentrations from an oxalate standard solution. A volume of approximately 10 mL
197 was used for each measurement and MQ water was used intermittently to flush the instrument
198 between each sample.

199 The pH of the cloud water samples was measured using an Orion Star^{TM} A211 pH meter with an
200 Orion^{TM} 8103BNUWP ROSS Ultra^{TM} pH electrode (precision of 0.01). A two-point calibration
201 (pH = 4 and pH = 7) was performed at the beginning of analyzing a particular flight's set of
202 samples.

203

2.3.3 Units

205 While many studies report concentrations in terms of air-equivalent concentrations, we instead
206 use the native liquid-phase concentrations. Aqueous concentrations of TOC and individual
207 molecular components are reported in units of ppb (i.e., parts per billion by mass). TOC
208 concentrations are specific to the mass of carbon atoms only, while molecules measured by IC
209 correspond to the specific mass of the species (unless noted otherwise). TOC was converted to
210 total organic matter (TOM) via multiplication by 1.8 (Zhang et al., 2005).

211 The choice to focus on aqueous- rather than air-equivalent concentrations was made for various
212 reasons. First, our analysis focuses heavily on relative amounts of species that were unaffected
213 by multiplying native aqueous units by cloud liquid water content. Second, the definition of
214 liquid water content applied by studies can vary widely based on the lower and upper bound of
215 what is considered a droplet. Third, relationships between solute concentrations in cloud water
216 and liquid water content, anticipated from nucleation scavenging, are ineffective when gases like
217 acetic and formic acids absorb directly into droplets rather than having been part of the initial
218 CCN activating into droplets (Khare et al., 1999; Marinoni et al., 2004). Lastly, many studies of
219 cloud water composition that our results can be contrasted with also use liquid units. The primary
220 liquid units reported for cloud water concentrations are ppm and ppb. However, it should be
221 noted that species concentrations in cloud water can be high simply due to the liquid water

222 content being low, or inversely the concentrations can be low due to being diluted by high liquid
223 water content.

224

225 **2.4 Aerosol Composition**

226 To complement the cloud water composition results, we use aerosol composition results from the
227 High-Resolution Time-of-Flight Aerosol Mass Spectrometer (AMS; Aerodyne, Inc.), which
228 reports non-refractory composition for the submicrometer range (DeCarlo et al., 2006). As
229 summarized by Hilario et al. (2021), the AMS deployed in CAMP^{2}Ex functioned in 1 Hz Fast-
230 MS mode with data averaged to 30 s time resolution with the lower limit of detection (units of
231 μg m^{-3}) as follows for the measured species: organic (0.169), NH_4^+ (0.169), SO_4^{2-} (0.039), NO_3^-
232 (0.035), Cl^- (0.036). Negative mass concentrations were recorded owing to the difference method
233 used with the limits of detection. These negative values were included in the analyses to avoid
234 positive biases but were interpreted as zero concentrations. We also use data specifically for the
235 mass spectral marker representative of acid-like oxygenated organic species (*m/z* 44=COO^+)
236 (Aiken et al., 2008) and its mass relative to total organic mass (f_{44}). AMS data were omitted from
237 analysis if total mass of all detected species was < 0.5 μg m^{-3}. By convention for airborne
238 sampling, AMS data are reported at standard temperature and pressure (STP; 273 K, 1013 hPa).

239 AMS data were reported separately for cloud-free and cloudy conditions owing to the use of a
240 counterflow virtual impactor (CVI) inlet (Brechtel Manufacturing Inc.) (Shingler et al., 2012) in
241 clouds to isolate and dry droplets, leaving the residual particles for sampling by the AMS. Cloud-
242 free data involve sampling with a separate inlet designed by the University of Hawaii
243 (McNaughton et al., 2007). For cloud-free AMS results, data were selected 60 seconds before
244 and after each cloud water sample's start and end time, respectively, when the aircraft was not in
245 cloud. CVI-AMS data were reported for data collected within the period of cloud water
246 collection. It should be noted that cloud-free AMS data are missing for some cloud water
247 samples when the CVI was still in use for the 60 s before and after a sample's start and end time,
248 respectively.

249

250 **2.5 HYSPLIT**

251 Air mass origination was determined using 5-day back trajectories from the National Oceanic
252 and Atmospheric Administration (NOAA) Hybrid Single Particle Lagrangian Integrated
253 Trajectory model (HYSPLIT) (Rolph et al., 2017; Stein et al., 2015). Trajectories were generated
254 at 1-minute temporal resolution with meteorological inputs from the Global Forecast System
255 (GFS) reanalysis with a horizontal resolution of $0.25° \times 0.25°$ using the "model vertical velocity"
256 method.

257

258 **2.6 NAAPS**

259 The Navy Aerosol Analysis and Prediction System (NAAPS) global aerosol model was
260 implemented to assist in identifying biomass burning cases (Lynch et al., 2016)
261 (https://www.nrlmry.navy.mil/aerosol/). NAAPS relies on global meteorological fields from the
262 Navy Global Environmental Model (NAVGEM) (Hogan and Brody, 1993; Hogan and Rosmond,
263 1991) that analyzes and forecasts a $1° \times 1°$ grid with 6-hour intervals with 24 vertical levels. In
264 terms of identifying biomass burning cases, surface smoke concentrations were examined.
265

266 **3. Cumulative Results**
267 **3.1 Concentration Statistics**

268 TOC values ranged from 0.018 – 13.66 ppm C, with median and mean concentrations of 0.546
269 and 0.902 ppm C, respectively (Table 1). Samples in this study exhibited nearly the lowest mean
270 TOC value of all cloud water studies surveyed in Fig. 1, with the other lowest values being over
271 the Pacific Ocean west of San Diego, California (0.85 ppm C), (Straub et al., 2007) and East
272 Peak, Puerto Rico (0.90 ppm C), (Gioda et al., 2008; Gioda et al., 2011; Reyes-Rodríguez et al.,
273 2009). The CAMP^{2}Ex dataset exhibited the lowest minimum TOC value of all shown studies.
274 For context, the highest mean and maximum TOC masses in cloud water studies were 34.5 and
275 51.7 ppm C, respectively, at Jeju Island, Korea, while the peak dissolved organic carbon (DOC)
276 mass in cloud water was 85.6 ppm C at Mt. Tai, China. For comparisons to published cloud
277 water measurements, DOC and TOC are assumed to be sufficiently similar in nature to directly
278 compare values. Differences in TOC between our study and others can partly be attributed to the
279 different types of clouds studied in the CAMP^{2}Ex region (e.g., cumulus congestus, cumulus,
280 altocumulus, altostratus) and the higher collection altitudes being conducive to enhanced liquid
281 water contents and droplet sizes than stratocumulus clouds in regions like the northeastern
282 (Straub et al., 2007) and southeastern Pacific Ocean (Benedict et al., 2012). Previous studies
283 have primarily sampled stratocumulus or stratus clouds (Fig. 1). Also, some of our samples may
284 have included rain water, which naturally has lower concentrations of TOC than cloud water due
285 to dilution (Fig. 1). To illustrate the importance of this dilution effect, an average of the mean
286 values from the Fig. 1 studies shows the following (ppm C): Fog = 17.8, cloud = 6.4, rain = 0.6.
287 We further note that direct comparisons of our results to others need to factor that water
288 collectors have different transmission efficiency behavior as a function of droplet size, as well as
289 compositional differences across the droplet size spectrum (i.e., Boris et al., 2016; Collett Jr. et
290 al., 2008; Herckes et al., 2013).

291 The order of species is as follows in terms of decreasing average contribution of C mass relative
292 to total TOC (± one standard deviation): acetate (14.7 ± 20.5%), formate (5.4 ± 9.3%), oxalate
293 (2.8 ± 4.3%), DMA (1.7 ± 6.3%), succinate (1.6 ± 2.4%), pyruvate (1.3 ± 4.5%), glycolate (1.3 ±
294 3.7%), adipate (1.0 ± 3.6%), MSA (0.1 ± 0.1%), glutarate (0.1 ± 0.2%), and maleate (< 0.1 ±
295 0.1%). An average of 70.0% of TOC mass went unaccounted for. The predominant sources and
296 production pathways of these species are briefly explained here. Precursor emissions sources for
297 acetate and formate include plants, soil, vehicles, and biomass burning, with key production
298 routes including oxidation of isoprene, ozonolysis of olefins, and peroxy radical reactions (Khare
299 et al., 1999, and references therein). Pyruvate is considered the most abundant aqueous reaction
300 product of methylglyoxal, generated by the oxidation of gas-phase anthropogenic volatile

301 organic compounds (Boris et al., 2014; Carlton et al., 2006; Lim et al., 2013; Stefan et al., 1996;
302 Tan et al., 2010). Glycolate has been linked to aqueous processing of acetate and a precursor for
303 glyoxylate (Boris et al., 2014) and formed via oxidation of glycolaldehyde by hydroxide radicals
304 (Thomas et al., 2016). Oxalate is the most abundant dicarboxylic acid across different
305 environments (Cruz et al., 2019; Stahl et al., 2020; Yang et al., 2014; Ziemba et al., 2011) and
306 can be emitted directly by biogenic sources (Kawamura and Kaplan, 1987), combustion exhaust
307 (Kawamura and Kaplan, 1987; Kawamura and Yasui, 2005), and biomass burning (Narukawa et
308 al., 1999; Yang et al., 2014); however, it is also formed through the oxidation and degradation of
309 longer chain organic acids and acts as a notable tracer for cloud processing (Ervens et al., 2004;
310 Sorooshian et al., 2006). Saturated organics like glutarate, adipate, and succinate are linked to
311 fresh emissions and mainly from ozonolysis of cyclic alkenes (such as from vehicular emissions)
312 in the study region (Hatakeyama et al., 1985; Stahl et al., 2020). Maleate can be secondarily
313 formed from the photooxidation of benzene (Rogge et al., 1993) or from the primary emissions
314 of combustion engines (Kawamura and Kaplan, 1987). Alkyl amines (i.e., DMA) have numerous
315 sources such as biomass burning, vehicular emissions, industrial activity, animal husbandry,
316 waste treatment, and the ocean (Youn et al., 2015). Finally, MSA is formed via photooxidation
317 reactions involving dimethylsulfide (DMS) from oceanic emissions (Berresheim, 1987; Saltzman
318 et al., 1983) or dimethyl sulfoxide (DMSO) from anthropogenic emissions (Yuan et al., 2004), in
319 addition to being linked to agricultural emissions and biomass burning (Sorooshian et al., 2015).

320 Measured organic species were further grouped into categories: monocarboxylic acids (MCA;
321 glycolate, acetate, formate, pyruvate), dicarboxylic acids (DCA; glutarate, adipate, succinate,
322 maleate, oxalate), and measured organics (MO = sum of MCA, DCA, MSA, DMA). Total MCA
323 concentrations accounted on average for ~75% of MO and were approximately four times larger
324 than those of DCAs. MO values ranged from 29.46 – 10820 ppb, accounting for an average of
325 30.0% (median 23.8%) of TOC when masses were converted to just the C masses of the
326 measured species (Table 1). Examples of other undetected organics include tricarboxylic acids,
327 aromatics, alcohols, sugars, carbohydrates, and aldehydes. Previous studies reported undetected
328 species accounting for ~45% (Boris et al., 2016) and 82.9% (Boris et al., 2018) of organics.
329 Interestingly, the ionic charge balance for the 159 samples show an anion deficit (Fig. S1), with a
330 slope of 0.95 (i.e., anion charge on y-axis). This strong charge balance suggests that detected
331 organic species were balanced by cations detected via IC analysis. Species contributing to the
332 anion deficit likely include a mix of unspeciated organic and inorganic anions.

333 TOC was converted to total organic matter (TOM) by multiplying it by 1.8 (Zhang et al., 2005),
334 as in other cloud water studies (Boris et al., 2016; Boris et al., 2018), in order to compare it to
335 total measured mass (i.e., sum of TOM, Na^+, NH_4^+, K^+, Mg^{2+}, Ca^{2+}, Cl^-, NO_2^-, Br^-, NO_3^-, SO_4^{2-}).
336 We caution that using a fixed 1.8 conversion value yields uncertainty as samples were collected
337 in a range of air masses, but 1.8 is a value fairly intermediate to those reported in the literature:
338 1.6 ± 0.2 for urban aerosols (Turpin and Lim, 2001), 2.07 ± 0.05 in nonurban areas (Yao et al.,
339 2016), and values for biomass burning organic aerosols ranging from 1.56 – 2.0 (Aiken et al.,
340 2008; Turpin and Lim, 2001) based on fuel type and combustion condition (Aiken et al., 2008).
341 Higher values are expected for more oxidized organics. Estimated TOM accounted for a median
342 and mean of 23.2% and 30.7%, respectively, of total measured mass, with the maximum for a

343 single sample being 95.1%. The median and mean ratios of MO to TOM were 38.1% and 46.4%,
344 respectively. Furthermore, the median and mean ratios of MO to total measured mass were 7.2%
345 and 10.3%, respectively, with a maximum of 57.6%. On average, chloride, sulfate, and nitrate
346 were the most abundant species ($\geq$ 12.6%), with the median and mean ratio of total inorganic
347 mass to TOM being 3.3 and 5.8, respectively. The pH of the cloud water with TOC
348 measurements ranged from 3.79 – 5.93 and averaged 5.04 $\pm$ 0.51. The lowest pH values all
349 occurred over the ocean.

350 Our calculated percentages of MO relative to total measured mass are in contrast to results from
351 a surface site in Metro Manila (Stahl et al., 2020), where most of the same organic species
352 (adipate, succinate, maleate, oxalate, MSA) accounted for ~1.3% of total aerosol mass, excluding
353 black carbon. Therefore, the first hypothesis of this study holds true that the contributions of
354 measured organic species account for a greater portion of total measured mass in cloud water as
355 compared to surface particulate matter.

356 Gravimetry was used to measure total mass in the surface measurements whereas in cloud water,
357 total measured mass was more restrictive in terms of being based on measurable species, thus
358 qualifying our percentages as an upper bound. However, the measured ions in cloud water should
359 contribute relatively more to total measured mass in cloud water owing to their hygroscopic
360 nature (e.g., sea salt) and greater ease to become associated with cloud water as compared to
361 more hydrophobic species (Chang et al., 2017; Dalirian et al., 2018; Pringle et al., 2010) like
362 black carbon that contribute significantly to total aerosol mass in the boundary layer of Metro
363 Manila (Cruz et al., 2019). For example, black carbon accounted for 78.1% and 51.8% of the
364 total mass between 0.10 – 0.18 μm and 0.18 – 0.32 μm in Metro Manila surface aerosol particles
365 (Cruz et al., 2019), respectively, size ranges of which are highly relevant to droplet activation.
366 Air masses aloft in the CAMP^{2}Ex region, and especially those processed by clouds, are likely
367 more aged and oxidized compared to fresh organic emissions (e.g., automobiles, industry,
368 burning) in the surface layer over Metro Manila, which is the most populated urban area within
369 the CAMP^{2}Ex flight domain. Recent work has shown that cloud processing of isoprene oxidation
370 products (a key fraction of organic precursor vapors involved with organic aerosol generation) is
371 the main source of secondary organic aerosol (SOA) in the mid-troposphere (4 – 6 km)
372 (Lamkaddam et al., 2021). This motivates examining vertical TOC and organic species
373 characteristics in more detail, which is discussed next.

374

375 **3.2 Vertical Profiles**

376 The vertical profile of TOC masses were of interest as it relates to general vertical distribution of
377 organic matter in the troposphere. Measurements off the coast of Japan approximately two
378 decades ago during the ACE-Asia campaign revealed unexpectedly high organic aerosol
379 concentrations in the free troposphere due to presumed SOA formation (Heald et al., 2005).
380 During that campaign, organic aerosol concentrations in the boundary layer and free troposphere,
381 and their relative contribution to total non-refractory aerosol mass (organic, SO_4^{2-}, NO_3^-, NH_4^+),
382 were amongst the highest of various global regions examined (Heald et al., 2011). Therefore, it is

383   of interest to examine such types of vertical profiles farther south in the CAMP^{2}Ex region where
384   data are more scarce, with the unique aspect of this work being the focus on cloud water
385   composition.

386   The highest TOC masses were observed in the bottom two kilometers, with a general reduction
387   above that altitude (Fig. 3). The decrease of TOC concentration with respect to altitude could be
388   attributed to more dilution in larger droplet sizes; results of cloud microphysical data will be the
389   focus of forthcoming work. Four data points influenced by biomass burning were singled out in
390   red markers (Fig. 3a) owing to having systematically higher TOC masses than other points.
391   Those points will be discussed in more detail in Sect. 4, and it is noteworthy that clouds were
392   impacted by biomass burning across a wide range of altitudes up to almost 7 km.

393   Focusing on the non-biomass burning (non-BB) data, there was considerable variation in the
394   bottom 2 km in TOC, with concentrations as low as 0.144 ppm C and as high as 3.362 ppm C.
395   Interestingly, cloud water collected above 5 km tended to still show enhanced TOC masses,
396   reaching up to 1.530 ppm C (6.1 km) among the non-BB points. The composition contributing to
397   TOC was similar with altitude in non-BB and biomass burning (BB) conditions, with ~75% of
398   TOC mass unaccounted for by the measured species, and MCAs dominating the measured
399   organic mass (Fig. 3b). The exception to that was the high-altitude BB point where 95.6% of
400   TOC was unassigned. Fig. 3c-d show that there was some qualitative agreement in the vertical
401   profile of AMS organic and m/z 44 for data collected immediately adjacent to the cloud water
402   samples in cloud-free air; more specifically, the highest concentrations of AMS organic, m/z 44,
403   and TOC were in the bottom 2 km. However, some interesting differences exist as they related to
404   specific air mass types as will be discussed in Sect. 4. Some differences could be rooted in how
405   AMS data represent submicrometer particles whereas cloud water data encompass a wider range
406   of particle sizes that activated into cloud droplets (including supermicrometer dust and sea salt
407   particles) and also gases partitioning to cloud water.

408   Vertical profiles of ratios representative of the relative amount of oxidized organics are shown in
409   Fig. 4. The MO:TOC ratio was quite variable with altitude ranging from 0.16 to 0.32 based on
410   the locally averaged curve shown; individual sample values ranged from 0.01 to 0.92. Vertically-
411   resolved ratio values for f_{44} in cloud-free air and in cloud (downstream CVI) ranged on average
412   between 0 to 0.35 and 0.13 to 0.35, respectively. While mass concentrations decreased with
413   altitude (Fig. 3), ratios relevant to the degree of organic aerosol oxidation and make-up of the
414   organic component of cloud water did not exhibit a clear change with altitude.

415

4. Case Studies

417   Four subsets of samples are examined here to probe how the organic nature of cloud water varies
418   for distinct air masses. Sources of the air masses are visually shown in Fig. 5 based on 5-day
419   HYSPLIT back-trajectories: (i) "North" (RF11, n = 20) collected off the northern coast of Luzon
420   with influence from East Asia, the Korean Peninsula, and Japan; (ii) "East" (RF13, n = 11)
421   collected off the eastern coast of Luzon with back-trajectories traced to southern China with
422   subsequent passage across Luzon before arriving to the area of sample collection; (iii) "Biomass

423 Burning" (RF09, n = 4) collected to the southwest of Luzon above the Sulu Sea with influence
424 from biomass burning plumes from Borneo and Sumatra primarily consisting of peat as the fuel
425 type (Field and Shen, 2008; Levine, 1999; Page et al., 2002; Stockwell et al., 2016; Xian et al.,
426 2013); and (iv) "Clark" (RF04, RF06, RF07, RF09, RF10, and RF11, n = 25) collected around
427 the operational area over Luzon, approximately ~90 km northwest of Metro Manila, with back-
428 trajectories extending to the west and southwest of Luzon.

429 Biomass burning samples were identified based on the following criteria: flight scientist notes,
430 elevated surface smoke concentrations and aerosol optical depth (AOD) from the NAAPS model,
431 and the remarkable enhancement in chemical concentrations in cloud water. TOC, K^+, SO_4^{2-}, and
432 NH_4^+ in particular were enhanced in these samples with concentrations exceeding 4 ppm C, 0.13
433 ppm, 2.3 ppm, and 2.5 ppm, respectively.

434 Vertical profile results shown previously (Figs. 3-4) show markers corresponding to these four
435 case studies. With the exception of one BB sample collected at 6.5 km, samples in the four cases
436 were obtained below 3.3 km.

437 **4.1 North**

438 This category of samples was unique in that the mean MO (527.5 ± 301.6 ppb) and TOC (636.1
439 ± 230.4 ppb C) concentrations were the lowest of all four cases (Table 2). The largest three
440 organic contributors to TOC (± one standard deviation) were acetate (177.8 ± 72.96 ppb C; 11.5
441 ± 4.0%), oxalate (148.7 ± 81.47 ppb C; 6.0 ± 1.3%), and formate (83.16 ± 79.65 ppb C; 3.0 ±
442 2.2%). Maleate and DMA were not detected for this case and 73.3% of the TOC went
443 unaccounted for. Samples in this category were collected between 1.2 and 2.9 km, without any
444 pronounced organic chemical trends with altitude (Figs. 3-4).

445 This case exhibited a few distinct features worth noting. First, it had the highest sea salt presence
446 based on the highest case-wide concentrations of Na^+ (3238 ± 2861 ppb), Cl^- (5277 ± 4333 ppb),
447 Mg^{2+} (347.1 ± 328.3 ppb), and Br^- (15.56 ± 8.036 ppb), the latter of which is a trace component
448 of sea salt (Seinfeld and Pandis, 2016). MSA originates partly from marine emissions of DMS,
449 but its concentration was among the lowest of all species for all four cases with a mass
450 contribution to total TOC (based on C mass) of only 0.17 ± 0.05% in the North category (Table
451 3). In their analysis of aerosol data in the surface layer of Metro Manila, Stahl et al. (2020)
452 showed lower overall organic acid aerosol concentrations in the northeast monsoon season where
453 northeasterly air masses originated predominantly from East Asia; Stahl et al. (2020) also
454 showed those air masses were characterized by an enhancement in organic acid masses in the
455 supermicrometer size range owing to adsorption to coarse particle types such as sea salt and dust,
456 but with a preference for dust (Mochida et al., 2003; Rinaldi et al., 2011; Sullivan and Prather,
457 2007; Turekian et al., 2003). As there was no direct evidence of dust in this case as the Ca^{2+}:Na^+
458 ratio was on average (0.04) nearly the same as sea salt (0.038) (Seinfeld and Pandis, 2016),
459 organic acids could have interacted with sea salt. There were strong correlations between sea salt
460 constituents, TOC, and almost all detected organics (Table S1).

461 The second notable feature of this case was limited air mass aging characteristics based on
462 speciated ratios. The acetate:formate ratio is often used to indicate the relative influence of fresh

463 emissions (higher ratios) as compared to secondary production (lower ratios) (Talbot et al., 1988;
464 Wang et al., 2007). In at least one study, fresh emissions were linked to cloud water ratios above
465 1.5 and aged samples having values below 1 (Coggon et al., 2014). The mean acetate:formate
466 ratio for this air mass category was 4.21 ± 3.26, which was the highest of all four categories in
467 Table 2, suggestive of fresh emissions and low aging. This was consistent with the $Cl^-:Na^+$ ratio
468 (1.70 ± 0.13) being the close to sea water (1.81); our use of this ratio in the study assumes these
469 species originate primarily from sea salt. Lower $Cl^-:Na^+$ values in the study region coincide with
470 sea salt reactions with acids such as sulfuric, nitric, and organic acids (AzadiAghdam et al.,
471 2019). This was one of the two cases that had adipate present, with this category exhibiting the
472 highest mean concentration $(5.146 \pm 6.266$ ppb). This suggests there was influence from cyclic
473 organics possibly originating from combustion sources, among others, during the transport to the
474 sample region. Adipate exhibited negative correlations with almost all other organic species in
475 this case (r: -0.48 – -0.72), suggestive of limited aging to form shorter chain carboxylic acids via
476 photochemical reactions (Table S1). With the exception of adipate, interrelationships between
477 the other organics detected in this case exhibited positive and significant correlations with one
478 another suggestive of common precursors and/or production mechanisms. Therefore, the results
479 of the North case point to influences from marine emissions and limited aging signatures based
480 on speciated ratios.

481

4.2 East

483 The dominant organic contributors to TOC $(1051 \pm 330.6$ ppb C) in the East case were the same
484 as the North case with the difference being the order after acetate ($\pm$ one standard deviation):
485 acetate $(359.0 \pm 40.71$ ppb; $14.9 \pm 3.1\%$), formate $(258.2 \pm 122.2$ ppb; $7.2 \pm 3.8\%$), and oxalate
486 $(153.6 \pm 81.06$ ppb; $3.8 \pm 1.2\%$). The percentage of TOC unaccounted for by the speciated
487 measurements (69.4%) was the lowest out of all of the cases. This case resembled the North one
488 in that there was marine influence, but with differences being more pronounced dust influence
489 and greater evidence of aging based on chemical ratios. Marine signatures come from the second
490 highest concentrations of Na^+, Cl^-, and Mg^{2+} after North, with high correlations between these
491 species (Table S2).

492 Unlike the previous case, the $Ca^{2+}:Na^+$ ratio (0.10) was elevated from that of typical sea salt
493 (0.038). Wang et al. (2018) showed that East Asian dust can get lofted up during dust storms,
494 which could contribute to the transport to the Philippines. Previous studies have shown that
495 organic acids adsorb more readily to dust as compared to sea salt due to dust's more alkaline
496 nature (Stahl et al., 2020; Sullivan and Prather, 2007). While Ca^{2+} was correlated to six of the 11
497 organic species for this case (r: 0.70 – 0.96; Table S2), the magnitude of the correlations was
498 very similar to those between either Na^+ or Cl^- and the speciated organics. TOC also exhibited
499 similar correlations with Na^+, Cl^-, and Ca^{2+} (r: 0.83 – 0.87). Therefore, it is too difficult with the
500 given data to assert whether (if at all) the organic acids had a preference towards either salt or
501 dust aerosol particles; of note though is that oxalate exhibited the strongest correlation with
502 either Na^+, Cl^-, and Ca^{2+} (r: 0.96 – 0.99) among all species and also TOC. Additionally, Park et
503 al. (2004) showed enhanced Ca^{2+} and NO_3^- in the coarse mode owing to continental Asian dust.

504 In the East case, speciated organics were fairly well correlated to NO_3^- (r: 0.68 – 0.99), which
505 has been associated with adsorption onto coarse aerosol types like dust and sea salt (e.g.,
506 Maudlin et al., 2015; Stahl et al., 2020). Nitrate was especially well correlated with Na^+, Cl^-, and
507 Ca^{2+} (r: 0.98 – 1.00), which exceeded correlations of other common inorganic ions such as SO_4^{2-}
508 and NH_4^+.

509 The vertical profiles show clearly the systematically higher TOC masses relative to the North
510 case across roughly the same altitude range (1.3 – 3.3 km), but in contrast the AMS organic and
511 m/z 44 values (although sparse) were more comparable, which again can simply be due to the
512 differences in what is being measured with AMS not accounting for the supermicrometer
513 particles types (i.e., dust and sea salt) that likely were more influential in the cloud water in the
514 East case. However, the importance of droplet uptake of water-soluble organic gases should also
515 be considered as they can influence TOC mass.

516 Evidence of greater aging as compared to the North case comes from a few ratios of interest. The
517 Cl^-:Na^+ ratio for this case (1.40 ± 0.06) was lower than the North case, suggestive of more sea
518 salt reactivity aided by presumed aging. Furthermore, the acetate:formate ratio (1.93 ± 1.51) was
519 less than half the value from the North case. More broadly, the overall contribution of MCAs and
520 DCAs to TOC were very similar between the North and East cases and also the next two cases:
521 MCA:TOC = 16.03% – 23.66%, and DCA:TOC = 3.70% – 8.75% (Table 3). In contrast to the
522 North case, this category of samples had weaker interrelationships between organic species
523 presumed to be due to the mixture of sources impacting this case including dust, marine
524 particles, and likely other anthropogenic and biogenic sources over land.

525

4.3 Biomass Burning

527 The BB category samples exhibited the highest concentrations of TOC (8342 ± 3730 ppb C) and
528 almost every organic with the dominant contributors to TOC (± one standard deviation) being
529 formate (2178 ± 1589 ppb; 7.0 ± 4.5%), acetate (1845 ± 1668 ppb; 8.4 ± 5.6%), and succinate
530 (557.0 ± 575.6 ppb; 2.4 ± 1.7%). As acetate and formate were so abundant, the relative
531 enhancement of MCA mass was much larger than DCA mass as compared to the three other
532 cases examined (Table 2). While the correlation matrix for this case was quite sparse in terms of
533 significant values owing partly to such few points (n = 4), TOC and K^+ were highly correlated (r:
534 0.99), which demonstrates the strong linkage between TOC and biomass burning emissions
535 (Table S3) as also shown by others (Cook et al., 2017). For context, Desyaterik et al. (2013)
536 reported cloud water TOC masses of 100.6 ppm C in a biomass burning airmass at Mt. Tai in
537 eastern China that was eight times higher than typical values in the absence of agricultural
538 burning. Cook et al. (2017) observed significant higher cloud water TOC masses during wildfire
539 periods at Whiteface Mountain, New York (16.6 ppm C) than biogenic (2.16 ppm C) or urban
540 (2.11 ppm C) periods.

541 In our BB samples, mean values of succinate (557.0 ± 575.6 ppb), glutarate (150.4 ± 82.20 ppb),
542 and pyruvate (125.9 ± 126.1 ppb) were significantly elevated above the other cases. Stahl et al.
543 (2020) recently showed that succinate, oxalate, and MSA were especially enhanced in aerosol

samples collected in the study region during BB periods in the 2018 southwest monsoon season. Study-wide peak concentrations of succinate (1372 ppb), oxalate (1135 ppb), and MSA (24.79 ppb) were found in this case reinforcing those findings (Stahl et al., 2020). Unlike the previous two cases, maleate was detected in BB samples (5.583 ± 6.456 ppb). Although maleate is associated with combustion sources (Kawamura and Kaplan, 1987; Rogge et al., 1993), such as from extensive ship traffic around the sampling area, other studies have shown enhancements of maleate in BB air masses (i.e., Mardi et al., 2019; Tsai et al., 2013). The percentage of mass contributing to TOC that was unaccounted for was 78.7%, with the highest sample at 6.5 km having 95.6% undetected, which was surprisingly large based on the prevalence of organic acids in biomass burning emissions (Reid et al., 1998). Therefore, the second hypothesis posed in this study is partly true in that the BB case exhibited much higher TOC values; however, these samples did not exhibit a greater contribution by organic acids to TOC since the North and East cases actually had a greater contribution from such species. This motivates more attention to organic chemical speciation in clouds impacted by biomass burning emissions as such a large portion of the TOC mass went unaccounted for in this study.

While absolute concentrations of most organics were greatly enhanced in BB, the relative contributions of individual organics within the MCA and DCA subsets of species also varied. Most notably in the MCA category, formate was greatly enhanced with a mass contribution to total MCA mass being 46.40% versus 16.54% – 29.09% for other cases. In the DCA population of species, glutarate and succinate accounted for higher mass fractions (17.15% and 41.95%) than other cases (0.65% – 4.02% and 20.82% – 38.52%, respectively).

The Cl^-:Na^+ ratio was 1.30 ± 0.06 and suggestive of Cl^- depletion, which has been observed in other regions with biomass burning and linked to high concentrations of inorganic and organic acids (Braun et al., 2017, and references therein). This is supported by how the values of MO, SO_4^{2-}, and NO^{3-} were the highest in this case (Table 2). The acetate:formate ratio was 0.69 ± 0.30, but it is unclear as to how effective this and other ratios are as aging indicators when biomass burning is present and especially as fuel type varies between regions. Talbot et al. (1988) and Wang et al. (2007) both report that the acetate:formate ratio is substantially larger in biomass burning samples, which is contradictory to the ratios that are reported for this case ranging from 0.32 – 1.03. This could be due to the fuel type or due to aging of the biomass burning plume, however this is speculatory and should be examined more extensively.

4.4 Clark

Samples in this category were collected during ascents after takeoff and descents during approaches to the airfield, which allowed for sample collection closer to the surface than the other categories (altitude range: 0.2 – 2.9 km). Clark International Airport is located within the Clark Freeport Zone, which is part of both the Pampanga and Tarlac provinces and consists of five cities and municipalities: Angeles City, Mabalacat City, Porac, Capas, and Bamban. This gives the Clark area a population of approximately 996,000 with a population density of ~3100 km^{-2}, which is low in comparison to the most populated city in the Philippines, Quezon City in

584 Metro Manila, with 2.94 million people and a population density of ~17000 km^{-2} (PSA, 2016). In
585 addition to Metro Manila just to the southeast (~90 km), Clark lies between Mt. Pinatubo to the
586 west and Mt. Arayat to the east, which are active and potentially active volcanoes, respectively.

587 The average TOC for this case (1181 ± 920.2 ppb C) was most similar to the East case and
588 exhibited the most variability relative to the mean TOC value of all four cases, which we
589 attribute to numerous sources impacting these samples including local and regional emissions,
590 time of day variability, local spatial variability, and number of flights. This case exhibited the
591 highest percentage of TOC mass unaccounted for by speciated organics (79.5%) with the three
592 largest measured contributors (± one standard deviation) consisting of acetate (296.7 ± 325.8
593 ppb; 9.6 ± 9.5%), formate (266.1 ± 316.8 ppb; 4.8 ± 3.3%), and oxalate (88.33 ± 103.9 ppb; 1.7
594 ± 1.0%). A few notable features are mentioned specific to this case. This was the only case that
595 had DMA present (6.454 ± 15.89 ppb) albeit with a low mass contribution to total TOC (0.43 ±
596 1.17%). This case exhibited the highest mass fractions of maleate (3.20 ± 5.93%) and adipate
597 (16.05 ± 21.48%) relative to DCA mass, suggestive of greater anthropogenic emission influence
598 and processed aromatic compounds. DMA was only correlated with maleate (r: 0.67) among the
599 organic species suggestive of a similar source (Table S4). Stahl et al. (2020) showed increased
600 aerosol concentrations of freshly emitted organics (i.e., phthalate, maleate) owing to the vast
601 sources of combustion engines to the southeast of the Clark area. Clark is situated near a major
602 highway that could also contribute to the high combustion sources, though commercial aircraft
603 emissions could also have a significant role.

604 Because succinate peaked in concentration for this case (498.50 ppb) and back-trajectories
605 originated from Borneo and Sumatra, there may have been some influence from biomass burning
606 (Fig. 5). The K^+:Na^+ ratio was elevated (0.25) above that of sea salt (0.036) (Seinfeld and Pandis,
607 2016), and even higher than the Biomass Burning case (0.15), suggestive of local and/or regional
608 biomass burning influence. This case exhibited the highest mean Ca^{2+}:Na^+ ratio (0.99) that was
609 well above the sea salt value (0.038), which we presume could be linked largely to resuspended
610 and/or transported dust. Cruz et al. (2019) showed for Metro Manila that resuspended dust,
611 especially linked to vehicular traffic, is an important source of dust in the study region. Stahl et
612 al. (2020) showed that adipate is most influenced by crustal sources in the study region and was
613 unique among the studied organics in this work in that it exhibited a prominent peak in the
614 supermicrometer range based on surface aerosol measurements in Metro Manila. Consistent with
615 that work, Ca^{2+} was only correlated with adipate in the Clark samples (r: 0.71) among the studied
616 organics (Table S4), adding support for how organic acids like adipate can partition to dust with
617 the novelty here being that the signature was observed in cloud water.

618

5. Conclusion

620 This work analyzed 159 cloud water samples collected over a 2-month period as part of the
621 CAMP^{2}Ex airborne campaign around the Philippines. TOC and a total of eleven organic
622 compounds comprised of four MCAs (glycolate, acetate, formate, and pyruvate), five DCAs
623 (glutarate, adipate, succinate, maleate, and oxalate), MSA, and DMA were measured. The

624 measured organics were then compared to TOC to determine the percentage of organic species
625 measured compared to the total organic composition. Notable results are summarized below
626 including responses to the two hypotheses proposed at the end of Sect. 1.

627 • TOC masses ranged widely between 0.018 – 13.66 ppm C between 0.2 – 6.8 km, with a
628   mean value of 0.902 ppm C. The contribution (in C mass) of the 11 measured species to
629   total TOC was on average 30%. Using a conversion factor of 1.8 for organic matter
630   relative to organic carbon, the mean amount of total organic matter (TOM) accounted for
631   by our measured 11 species was 46.4%. Furthermore, the mean contribution of TOM and
632   speciated organics to total mass (inorganics + organics) was 30.7% (maximum = 95.1%)
633   and 10.3% (maximum = 57.6%), respectively. The mean ratio of inorganic to TOM was
634   5.8. The study's first hypothesis holds true that the measured organic species account for
635   a higher mass fraction relative to total mass as compared to surface layer aerosol
636   measurements over Luzon, excluding black carbon (~1.3%), (Stahl et al., 2020). This is
637   likely owing to more processed air masses aloft and the reduced influence of black
638   carbon that is so abundant in areas like Metro Manila (Cruz et al., 2019; Hilario et al.,
639   2020a). The uptake of water-soluble gases can also attribute to greater organic mass
640   contributions.

641 • In terms of the chemical profile of the speciated organics, the order in decreasing
642   contribution of C mass relative to TOC was as follows ($\pm$ one standard deviation): acetate
643   ($14.7 \pm 20.5\%$), formate ($5.4 \pm 9.3\%$), oxalate ($2.8 \pm 4.3\%$), DMA ($1.7 \pm 6.3\%$), succinate
644   ($1.6 \pm 2.4\%$), pyruvate ($1.3 \pm 4.5\%$), glycolate ($1.3 \pm 3.7\%$), adipate ($1.0 \pm 3.6\%$), MSA
645   ($0.1 \pm 0.1\%$), glutarate ($0.1 \pm 0.2\%$), maleate ($< 0.1 \pm 0.1\%$). Approximately 70.0% of
646   TOC went unaccounted for pointing to the complexity and difficulty of organic
647   speciation in the study region, with this value fairly similar to other regions too (Benedict
648   et al., 2012; Boris et al., 2016; Boris et al., 2018; Herckes et al., 2002; Raja et al., 2008).
649   Monocarboxylic acids dominated the speciated organic mass (~75%) and were about four
650   times more abundant than dicarboxylic acids, suggestive of higher abundance of gaseous
651   species and precursors. It should also be noted that MCAs have a higher volatility than
652   DCAs, which could contribute to the higher organic mass. Additionally, the MCAs
653   measured in this study were predominately short chain organics that have naturally higher
654   volatilities (Chebbi and Carlier, 1996; Wang et al., 2007).

655 • Vertical profiles of TOC revealed higher concentrations in the bottom 2 km with a
656   reduction above that. Samples impacted by biomass burning emissions were substantially
657   enhanced in TOC and most speciated organic masses, ranging in altitude from as low as
658   1.3 km to as high as 6.5 km. While vertical profiles of AMS organic and m/z 44 mass
659   concentrations qualitatively resembled that of TOC with reductions above 2 km, the
660   vertical behavior of chemical ratios relevant to the composition of the cloud (ratio of C
661   mass from measured organics to TOC) and aerosol organics (f_{44}) did not reveal any clear
662   trend. For both non-BB and BB samples, monocarboxylic acids uniformly dominated C
663   mass with ~75% of TOC mass unaccounted for across the range of altitudes studied.

664 • The second hypothesis in this study proved to be partly true as clouds impacted by
665   biomass burning exhibited markedly higher values of TOC (4.974 – 13.66 ppm C) and

666   masses of most all other species detected as compared to the other three categories of
667   samples in Sect. 4 (North, East, Clark). However, the part of the hypothesis about
668   speciated organic acids contributing more to BB samples did not hold true as total
669   measured organics accounted on average for 21.25% of the TOC, which was lower than
670   two of the other categories of samples (North [26.72%] and East [30.61%]). Interestingly,
671   the highest BB sample (6.5 km) had 95.6% of the C mass unaccounted for by speciated
672   organics. This motivates increased attention to organic speciation in clouds impacted by
673   biomass burning.

674   • Four categories of samples with different air mass history characteristics were compared
675   revealing a few notable features: (i) while speciated concentrations and TOC masses
676   varied considerably between the four cases, the contributions of MCAs and DCAs (based
677   on C mass) to TOC were remarkably similar with little variation (MCA:TOC = 16.03% –
678   23.66%, DCA:TOC and 3.70% – 8.75%); (ii) dust and sea salt tracer species were
679   strongly correlated to most all speciated organics for the North and East cases suggestive
680   of interactions between such species and coarse aerosol surfaces as supported by past
681   work (Stahl et al., 2020; Sullivan and Prather, 2007); (iii) for samples with limited aging
682   (North case) based on selected chemical ratio values, adipate was more abundant and
683   negatively correlated to smaller carboxylic acids; (iv) BB samples exhibited the highest
684   TOC concentrations (8342 ± 3730 ppb C) as well as significant elevations in individual
685   organics such as acetate, formate, succinate, glutarate, pyruvate, oxalate, and MSA; and
686   (v) the Clark case had a higher variability of TOC (1181 ± 920.2 ppb C) compared to the
687   North and East cases presumably owing to a greater mix of influential sources such as
688   fresh anthropogenic emissions (e.g., enhanced maleate), but also transport of biomass
689   burning plumes from Borneo and Sumatra (e.g., enhanced succinate), dust, as well as
690   spatial and temporal variances across different flights. Related to dust, Ca^{2+} was only
691   correlated to adipate in the Clark samples, consistent with a recent study in Metro Manila
692   (Stahl et al., 2020) showing that adipate uniquely exhibits a prominent supermicrometer
693   peak among organic acids attributed to interactions with dust.

694

Data availability

696   All data used can be found on the NASA data repository at
697   DOI:10.5067/Suborbital/CAMP2EX2018/DATA001.

698

Author contributions

700   EC, RAB, CS, ABM, and AS designed the experiment. All coauthors carried out various aspects
701   of the data collection. EC, CS, and AS conducted analysis and interpretation of the data. CS and
702   AS prepared the manuscript with contributions from the coauthors.

703

Competing interests

705   The authors declare that they have no conflict of interest.

706

Acknowledgements

708   The authors acknowledge support from NASA grant 80NSSC18K0148 in support of the NASA
709   CAMP^{2}Ex project. R. A. Braun acknowledges support from the ARCS Foundation. M. Cruz
710   acknowledges support from the Philippine Department of Science and Technology's ASTHRD
711   Program. A. B. MacDonald acknowledges support from the Mexican National Council for
712   Science and Technology (CONACYT).

713

References

715   Aiken, A. C., Decarlo, P. F., Kroll, J. H., Worsnop, D. R., Huffman, J. A., Docherty, K. S.,
716   Ulbrich, I. M., Mohr, C., Kimmel, J. R., Sueper, D., Sun, Y., Zhang, Q., Trimborn, A.,
717   Northway, M., Ziemann, P. J., Canagratna, M. R., Onasch, T. B., Alfarra, M. R., Prevot, A. S.
718   H., Dommen, J., Duplissy, J., Metzger, A., Baltensperger, U., and Jimenez, J. L.: O/C and
719   OM/OC ratios of primary, secondary, and ambient organic aerosols with high-resolution time-of-
720   flight aerosol mass spectrometry, Environ. Sci. Technol., 42, 4478-4485, 10.1021/es703009q,
721   2008.

722   Anastasio, C., Faust, B. C., and Allen, J. M.: Aqueous phase photochemical formation of
723   hydrogen peroxide in authentic cloud waters, J. Geophys. Res. Atmos., 99, 8231-8248,
724   10.1029/94JD00085, 1994.

725   AzadiAghdam, M., Braun, R. A., Edwards, E.-L., Bañaga, P. A., Cruz, M. T., Betito, G.,
726   Cambaliza, M. O., Dadashazar, H., Lorenzo, G. R., Ma, L., MacDonald, A. B., Nguyen, P.,
727   Simpas, J. B., Stahl, C., and Sorooshian, A.: On the nature of sea salt aerosol at a coastal
728   megacity: Insights from Manila, Philippines in Southeast Asia, Atmos. Environ., 216, 116922,
729   10.1016/j.atmosenv.2019.116922, 2019.

730   Barth, M., Rasch, P., Kiehl, J., Benkovitz, C., and Schwartz, S.: Sulfur chemistry in the National
731   Center for Atmospheric Research Community Climate Model: Description, evaluation, features,
732   and sensitivity to aqueous chemistry, J. Geophys. Res. Atmos., 105, 1387-1415,
733   10.1029/1999JD900773, 2000.

734   Benedict, K. B., Lee, T., and Collett Jr, J. L.: Cloud water composition over the southeastern
735   Pacific Ocean during the VOCALS regional experiment, Atmos. Environ., 46, 104-114,
736   10.1016/j.atmosenv.2011.10.029, 2012.

737   Berresheim, H.: Biogenic sulfur emissions from the Subantarctic and Antarctic Oceans, J.
738   Geophys. Res. Atmos., 92, 13245-13262, 10.1029/JD092iD11p13245, 1987.

739   Boris, A., Lee, T., Park, T., Choi, J., Seo, S., and Collett Jr., J.: Fog composition at Baengnyeong
740   Island in the eastern Yellow Sea: detecting markers of aqueous atmospheric oxidations, Atmos.
741   Chem. Phys., 16, 437-453, 10.5194/acp-16-437-2016, 2016.

742 Boris, A. J., Desyaterik, Y., and Collett Jr., J. L.: How do components of real cloud water affect
743 aqueous pyruvate oxidation?, Atmos. Res., 143, 95-106, 10.1016/j.atmosres.2014.02.004, 2014.

744 Boris, A. J., Napolitano, D. C., Herckes, P., Clements, A. L., and Collett Jr., J. L.: Fogs and air
745 quality on the southern California coast, Aerosol Air Qual. Res., 18, 224-239,
746 10.4209/aaqr.2016.11.0522 2018.

747 Braun, R. A., Dadashazar, H., MacDonald, A. B., Aldhaif, A. M., Maudlin, L. C., Crosbie, E.,
748 Aghdam, M. A., Mardi, A. H., and Sorooshian, A.: Impact of wildfire emissions on chloride and
749 bromide depletion in marine aerosol particles, Environ. Sci. Technol., 51, 9013-9021,
750 10.1021/acs.est.7b02039, 2017.

751 Braun, R. A., Aghdam, M. A., Bañaga, P. A., Betito, G., Cambaliza, M. O., Cruz, M. T.,
752 Lorenzo, G. R., MacDonald, A. B., Simpas, J. B., Stahl, C., and Sorooshian, A.: Long-range
753 aerosol transport and impacts on size-resolved aerosol composition in Metro Manila, Philippines,
754 Atmos. Chem. Phys., 20, 2387-2405, 10.5194/acp-20-2387-2020, 2020.

755 Capel, P. D., Gunde, R., Zuercher, F., and Giger, W.: Carbon speciation and surface tension of
756 fog, Environ. Sci. Technol., 24, 722-727, 10.1021/es00075a017, 1990.

757 Carlton, A. G., Turpin, B. J., Lim, H.-J., Altieri, K. E., and Seitzinger, S.: Link between isoprene
758 and secondary organic aerosol (SOA): Pyruvic acid oxidation yields low volatility organic acids
759 in clouds, Geophys. Res. Lett., 33, L06822, 10.1029/2005gl025374, 2006.

760 Chang, D., Lelieveld, J., Tost, H., Steil, B., Pozzer, A., and Yoon, J.: Aerosol physicochemical
761 effects on CCN activation simulated with the chemistry-climate model EMAC, Atmos. Environ.,
762 162, 127-140, 10.1016/j.atmosenv.2017.03.036, 2017.

763 Chebbi, A., and Carlier, P.: Carboxylic acids in the troposphere, occurrence, sources, and sinks:
764 A review, Atmos Environ, 30, 4233-4249, 10.1016/1352-2310(96)00102-1, 1996.

765 Coggon, M., Sorooshian, A., Wang, Z., Craven, J., Metcalf, A., Lin, J., Nenes, A., Jonsson, H.,
766 Flagan, R., and Seinfeld, J.: Observations of continental biogenic impacts on marine aerosol and
767 clouds off the coast of California, J. Geophys. Res. Atmos., 119, 6724-6748,
768 10.1002/2013JD021228, 2014.

769 Collett Jr., J. L., Hoag, K. J., Sherman, D. E., Bator, A., and Richards, L. W.: Spatial and
770 temporal variations in San Joaquin Valley fog chemistry, Atmos. Environ., 33, 129-140,
771 10.1016/S1352-2310(98)00136-8, 1998.

772 Collett Jr., J. L., Herckes, P., Youngster, S., and Lee, T.: Processing of atmospheric organic
773 matter by California radiation fogs, Atmos. Res., 87, 232-241, 10.1016/j.atmosres.2007.11.005,
774 2008.

775 Cook, R. D., Lin, Y.-H., Peng, Z., Boone, E., Chu, R. K., Dukett, J. E., Gunsch, M. J., Zhang,
776 W., Tolic, N., Laskin, A., and Pratt, K. A.: Biogenic, urban, and wildfire influences on the
777 molecular composition of dissolved organic compounds in cloud water, Atmos. Chem. Phys., 17,
778 10.5194/acp-17-15167-2017, 2017.

779 Crosbie, E., Brown, M. D., Shook, M., Ziemba, L., Moore, R. H., Shingler, T., Winstead, E.,
780 Thornhill, K. L., Robinson, C., MacDonald, A. B., Dadashazar, H., Sorooshian, A., Beyersdorf,
781 A., Eugene, A., Collett Jr., J., Straub, D., and Anderson, B.: Development and characterization of
782 a high-efficiency, aircraft-based axial cyclone cloud water collector, Atmos. Meas. Tech., 11,
783 5025-5048, 10.5194/amt-11-5025-2018, 2018.

784 Cruz, M. T., Bañaga, P. A., Betito, G., Braun, R. A., Stahl, C., Aghdam, M. A., Cambaliza, M.
785 O., Dadashazar, H., Hilario, M. R., Lorenzo, G. R., Ma, L., MacDonald, A. B., Pabroa, P. C.,
786 Yee, J. R., Simpas, J. B., and Sorooshian, A.: Size-resolved composition and morphology of
787 particulate matter during the southwest monsoon in Metro Manila, Philippines, Atmos. Chem.
788 Phys., 19, 10675-10696, 10.5194/acp-19-10675-2019, 2019.

789 Dalirian, M., Ylisirniö, A., Buchholz, A., Schlesinger, D., Ström, J., Virtanen, A., and Riipinen,
790 I.: Cloud droplet activation of black carbon particles coated with organic compounds of varying
791 solubility, Atmos. Chem. Phys., 18, 12477-12489, 10.5194/acp-18-12477-2018, 2018.

792 DeCarlo, P. F., Kimmel, J. R., Trimborn, A., Northway, M. J., Jayne, J. T., Aiken, A. C., Gonin,
793 M., Fuhrer, K., Horvath, T., Docherty, K. S., Worsnop, D. R., and Jimenez, J. L.: Field-
794 deployable, high-resolution, time-of-flight aerosol mass spectrometer, Anal. Chem., 78, 8281-
795 8289, 10.1021/ac061249n, 2006.

796 Decesari, S., Facchini, M., Fuzzi, S., McFiggans, G., Coe, H., and Bower, K.: The water-soluble
797 organic component of size-segregated aerosol, cloud water and wet depositions from Jeju Island
798 during ACE-Asia, Atmos. Environ., 39, 211-222, 10.1016/j.atmosenv.2004.09.049, 2005.

799 Deguillaume, L., Charbouillot, T., Joly, M., Vaïtilingom, M., Parazols, M., Marinoni, A., Amato,
800 P., Delort, A.-M., Vinatier, V., Flossmann, A., Chaumerliac, N., Pichon, J. M., Houdier, S., Laj,
801 P., Sellegri, K., Colomb, A., Brigante, M., and Mailhot, G.: Classification of clouds sampled at
802 the puy de Dôme (France) based on 10 yr of monitoring of their physicochemical properties,
803 Atmos. Chem. Phys., 14, 1485-1506, 10.5194/acp-14-1485-2014, 2014.

804 Desyaterik, Y., Sun, Y., Shen, X., Lee, T., Wang, X., Wang, T., and Collett Jr., J. L.: Speciation
805 of "brown" carbon in cloud water impacted by agricultural biomass burning in eastern China, J.
806 Geophys. Res. Atmos., 118, 7389-7399, 10.1002/jgrd.50561, 2013.

807 Ehrenhauser, F. S., Khadapkar, K., Wang, Y., Hutchings, J. W., Delhomme, O., Kommalapati,
808 R. R., Herckes, P., Wornat, M. J., and Valsaraj, K. T.: Processing of atmospheric polycyclic
809 aromatic hydrocarbons by fog in an urban environment, J. Environ. Monitor., 14, 2566-2579,
810 10.1039/C2EM30336A, 2012.

811 Erel, Y., Pehkonen, S. O., and Hoffmann, M. R.: Redox chemistry of iron in fog and stratus
812 clouds, J. Geophys. Res. Atmos., 98, 18423-18434, 10.1029/93JD01575, 1993.

813 Ervens, B., Feingold, G., Clegg, S. L., and Kreidenweis, S. M.: A modeling study of aqueous
814 production of dicarboxylic acids: 2. Implications for cloud microphysics, J. Geophys. Res.
815 Atmos., 109, D15206, 10.1029/2004jd004575, 2004.

816   Ervens, B., Wang, Y., Eagar, J., Leaitch, W., Macdonald, A., Valsaraj, K., and Herckes, P.:
817   Dissolved organic carbon (DOC) and select aldehydes in cloud and fog water: the role of the
818   aqueous phase in impacting trace gas budgets, Atmos. Chem. Phys., 13, 5117-5135,
819   10.5194/acp-13-5117-2013, 2013.

820   Ervens, B.: Modeling the processing of aerosol and trace gases in clouds and fogs, Chem. Rev.,
821   115, 4157-4198, 10.1021/cr5005887, 2015.

822   Faloona, I.: Sulfur processing in the marine atmospheric boundary layer: A review and critical
823   assessment of modeling uncertainties, Atmos. Environ., 43, 2841-2854,
824   10.1016/j.atmosenv.2009.02.043, 2009.

825   Field, R. D., and Shen, S. S.: Predictability of carbon emissions from biomass burning in
826   Indonesia from 1997 to 2006, J. Geophys. Res. Biogeosci., 113, G04024,
827   10.1029/2008JG000694, 2008.

828   Gelencser, A., Sallai, M., Krivacsy, Z., Kiss, G., and Meszaros, E.: Voltammetric evidence for
829   the presence of humic-like substances in fog water, Atmos. Res., 54, 157-165, 10.1016/S0169-
830   8095(00)00042-9, 2000.

831   Gioda, A., Mayol-Bracero, O. L., Reyes-Rodriguez, G. J., Santos-Figueroa, G., and Collett Jr., J.
832   L.: Water-soluble organic and nitrogen levels in cloud and rainwater in a background marine
833   environment under influence of different air masses, J. Atmos. Chem., 61, 85-99,
834   10.1007/s10874-009-9125-6, 2008.

835   Gioda, A., Reyes-Rodríguez, G. J., Santos-Figueroa, G., Collett Jr., J. L., Decesari, S., Ramos,
836   M. d. C. K., Bezerra Netto, H. J., de Aquino Neto, F. R., and Mayol-Bracero, O. L.: Speciation
837   of water-soluble inorganic, organic, and total nitrogen in a background marine environment:
838   Cloud water, rainwater, and aerosol particles, J. Geophys. Res. Atmos., 116, D05203,
839   10.1029/2010JD015010, 2011.

840   Hadi, D., Crossley, A., and Cape, J.: Particulate and dissolved organic carbon in cloud water in
841   southern Scotland, Environ. Pollut., 88, 299-306, 10.1016/0269-7491(95)93443-4, 1995.

842   Hallquist, M., Wenger, J. C., Baltensperger, U., Rudich, Y., Simpson, D., Claeys, M., Dommen,
843   J., Donahue, N., George, C., Goldstein, A., Hamilton, J. F., Herrmann, H., Hoffmann, T., Iinuma,
844   Y., Jang, M., Jenkin, M. E., Jimenez, J. L., Kiendler-Scharr, A., Maenhaut, W., McFiggans, G.,
845   Mentel, T. F., Monod, A., Prevot, A. S. H., Seinfeld, J. H., Surratt, J. D., Szmigielski, R., and
846   Wildt, J.: The formation, properties and impact of secondary organic aerosol: current and
847   emerging issues, Atmos. Chem. Phys., 9, 5155-5236, 10.5194/acp-9-5155-2009, 2009.

848   Hatakeyama, S., Tanonaka, T., Weng, J., Bandow, H., Takagi, H., and Akimoto, H.: Ozone-
849   cyclohexene reaction in air: quantitative analysis of particulate products and the reaction
850   mechanism, Environ. Sci. Technol., 19, 935-942, 10.1021/es00140a008, 1985.

851   Heald, C., Coe, H., Jimenez, J., Weber, R., Bahreini, R., Middlebrook, A., Russell, L., Jolleys,
852   M., Fu, T.-M., Allan, J., Bower, K. N., Capes, G., Crosier, J., Morgan, W. T., Robinson, N. H.,
853   Williams, P. I., Cubison, M. J., DeCarlo, P. F., and Dunlea, E. J.: Exploring the vertical profile of

854 atmospheric organic aerosol: comparing 17 aircraft field campaigns with a global model, Atmos.
855 Chem. Phys., 11, 12673-12696, 10.5194/acp-11-12673-2011, 2011.

856 Heald, C. L., Jacob, D. J., Park, R. J., Russell, L. M., Huebert, B. J., Seinfeld, J. H., Liao, H., and
857 Weber, R. J.: A large organic aerosol source in the free troposphere missing from current
858 models, Geophys. Res. Lett., 32, L18809, 10.1029/2005GL023831, 2005.

859 Herckes, P., Hannigan, M. P., Trenary, L., Lee, T., and Collett Jr., J. L.: Organic compounds in
860 radiation fogs in Davis (California), Atmos. Res., 64, 99-108, 10.1016/S0169-8095(02)00083-2,
861 2002.

862 Herckes, P., Chang, H., Lee, T., and Collett Jr., J. L.: Air pollution processing by radiation fogs,
863 Water Air Soil Pollut., 181, 65-75, 10.1007/s11270-006-9276-x, 2007.

864 Herckes, P., Valsaraj, K. T., and Collett Jr., J. L.: A review of observations of organic matter in
865 fogs and clouds: Origin, processing and fate, Atmos. Res., 132-133, 434-449,
866 10.1016/j.atmosres.2013.06.005, 2013.

867 Hilario, M. R. A., Cruz, M. T., Bañaga, P. A., Betito, G., Braun, R. A., Stahl, C., Cambaliza, M.
868 O., Lorenzo, G. R., MacDonald, A. B., AzadiAghdam, M., Pabroa, P. C., Yee, J. R., Simpas, J.
869 B., and Sorooshian, A.: Characterizing weekly cycles of particulate matter in a coastal megacity:
870 The importance of a seasonal, size-resolved, and chemically-speciated analysis, J. Geophys. Res.
871 Atmos., 125, e2020JD032614, 10.1029/2020JD032614, 2020a.

872 Hilario, M. R. A., Cruz, M. T., Cambaliza, M. O. L., Reid, J. S., Xian, P., Simpas, J. B.,
873 Lagrosas, N. D., Uy, S. N. Y., Cliff, S., and Zhao, Y.: Investigating size-segregated sources of
874 elemental composition of particulate matter in the South China Sea during the 2011 Vasco
875 cruise, Atmos. Chem. Phys., 20, 1255-1276, 10.5194/acp-20-1255-2020, 2020b.

876 Hilario, M. R. A., Crosbie, E., Shook, M., Reid, J. S., Cambaliza, M. O. L., Simpas, J. B. B.,
877 Ziemba, L., DiGangi, J. P., Diskin, G. S., Nguyen, P., Turk, F. J., Winstead, E., Robinson, C. E.,
878 Wang, J., Zhang, J., Wang, Y., Yoon, S., Flynn, J., Alvarez, S. L., Behrangi, A., and Sorooshian,
879 A.: Measurement report: Long-range transport patterns into the tropical northwest Pacific during
880 the CAMP2Ex aircraft campaign: chemical composition, size distributions, and the impact of
881 convection, Atmos. Chem. Phys., 21, 3777-3802, 10.5194/acp-21-3777-2021, 2021.

882 Hogan, T. F., and Rosmond, T. E.: The description of the Navy Operational Global Atmospheric
883 Prediction System's spectral forecast model, Mon. Weather Rev., 119, 1786-1815, 10.1175/1520-
884 0493(1991)119<1786:TDOTNO>2.0.CO;2, 1991.

885 Hogan, T. F., and Brody, L. R.: Sensitivity studies of the Navy's global forecast model
886 parameterizations and evaluation of improvements to NOGAPS, Mon. Weather Rev., 121, 2373-
887 2395, 10.1175/1520-0493(1993)121<2373:SSOTNG>2.0.CO;2, 1993.

888 Hutchings, J. W., Robinson, M. S., McIlwraith, H., Kingston, J. T., and Herckes, P.: The
889 chemistry of intercepted clouds in Northern Arizona during the North American monsoon
890 season, Water Air Soil Pollut., 199, 191-202, 10.1007/s11270-008-9871-0, 2008.

891   IPCC: Climate Change 2013: The Physical Science Basis, Cambridge University Press,
892   10.1017/CBO9781107415324, 2013.

893   Kanakidou, M., Seinfeld, J., Pandis, S., Barnes, I., Dentener, F. J., Facchini, M. C., Dingenen, R.
894   V., Ervens, B., Nenes, A., Nielsen, C., Swietlicki, E., Putaud, J. P., Balkanski, Y., Fuzzi, S.,
895   Horth, J., Moortgat, G. K., Winterhalter, R., Myhre, C. E. L., Tsigaridis, K., Vignati, E.,
896   Stephanou, E. G., and Wilson, J.: Organic aerosol and global climate modelling: a review,
897   Atmos. Chem. Phys., 5, 1053-1123, 10.5194/acp-5-1053-2005, 2005.

898   Kawamura, K., and Kaplan, I. R.: Motor exhaust emissions as a primary source for dicarboxylic
899   acids in Los Angeles ambient air, Environ. Sci. Technol., 21, 105-110, 10.1021/es00155a014,
900   1987.

901   Kawamura, K., and Yasui, O.: Diurnal changes in the distribution of dicarboxylic acids,
902   ketocarboxylic acids and dicarbonyls in the urban Tokyo atmosphere, Atmos. Environ., 39,
903   1945-1960, 10.1016/j.atmosenv.2004.12.014, 2005.

904   Khare, P., Kumar, N., Kumari, K., and Srivastava, S.: Atmospheric formic and acetic acids: An
905   overview, Rev. Geophy., 37, 227-248, 10.1029/1998RG900005, 1999.

906   Kim, H. J., Lee, T., Park, T., Park, G., Collett Jr., J. L., Park, K., Ahn, J. Y., Ban, J., Kang, S.,
907   Kim, K., Park, S.-M., Jho, E. H., and Choi, Y.: Ship-borne observations of sea fog and rain
908   chemistry over the North and South Pacific Ocean, J. Atmos. Chem., 76, 315-326,
909   10.1007/s10874-020-09403-8, 2020.

910   Kreidenweis, S. M., Walcek, C. J., Feingold, G., Gong, W., Jacobson, M. Z., Kim, C. H., Liu, X.,
911   Penner, J. E., Nenes, A., and Seinfeld, J. H.: Modification of aerosol mass and size distribution
912   due to aqueous-phase SO2 oxidation in clouds: Comparisons of several models, J. Geophys. Res.
913   Atmos., 108, 4213, 10.1029/2002JD002697, 2003.

914   Lamkaddam, H., Dommen, J., Ranjithkumar, A., Gordon, H., Wehrle, G., Krechmer, J., Majluf,
915   F., Salionov, D., Schmale, J., Bjelić, S., Carslaw, K. S., Haddad, I. E., and Baltensperger, U.:
916   Large contribution to secondary organic aerosol from isoprene cloud chemistry, Science
917   Advances, 7, eabe2952, 10.1126/sciadv.abe2952, 2021.

918   Levine, J. S.: The 1997 fires in Kalimantan and Sumatra, Indonesia: Gaseous and particulate
919   emissions, Geophys. Res. Lett., 26, 815-818, 10.1029/1999GL900067, 1999.

920   Li, J., Wang, X., Chen, J., Zhu, C., Li, W., Li, C., Liu, L., Xu, C., Wen, L., Xue, L., Wang, W.,
921   Ding, A., and Herrmann, H.: Chemical composition and droplet size distribution of cloud at the
922   summit of Mount Tai, China, Atmos. Chem. Phys., 17, 9885-9896, 10.5194/acp-17-9885-2017,
923   2017.

924   Lim, Y., Tan, Y., and Turpin, B.: Chemical insights, explicit chemistry, and yields of secondary
925   organic aerosol from OH radical oxidation of methylglyoxal and glyoxal in the aqueous phase,
926   Atmos. Chem. Phys., 13, 8651-8667, 10.5194/acp-13-8651-2013, 2013.

Liu, T., Chan, A. W., and Abbatt, J. P.: Multiphase oxidation of sulfur dioxide in aerosol particles: Implications for sulfate formation in polluted environments, Environ. Sci. Technol., 55, 4227-4242, 10.1021/acs.est.0c06496, 2021.

Löflund, M., Kasper-Giebl, A., Schuster, B., Giebl, H., Hitzenberger, R., and Puxbaum, H.: Formic, acetic, oxalic, malonic and succinic acid concentrations and their contribution to organic carbon in cloud water, Atmos. Environ., 36, 1553-1558, 10.1016/S1352-2310(01)00573-8, 2002.

Lynch, P., Reid, J. S., Westphal, D. L., Zhang, J., Hogan, T. F., Hyer, E. J., Curtis, C. A., Hegg, D. A., Shi, Y., Campbell, J. R., Rubin, J. I., Sessions, W. R., Turk, F. J., and Walker, A. L.: An 11-year global gridded aerosol optical thickness reanalysis (v1.0) for atmospheric and climate sciences, Geosci. Model Dev., 9, 1489-1522, 10.5194/gmd-9-1489-2016, 2016.

Ma, L., Dadashazar, H., Hilario, M. R. A., Cambaliza, M. O., Lorenzo, G. R., Simpas, J. B., Nguyen, P., and Sorooshian, A.: Contrasting wet deposition composition between three diverse islands and coastal North American sites, Atmos. Environ., 244, 117919, 10.1016/j.atmosenv.2020.117919, 2021.

MacDonald, A. B., Hossein Mardi, A., Dadashazar, H., Azadi Aghdam, M., Crosbie, E., Jonsson, H. H., Flagan, R. C., Seinfeld, J. H., and Sorooshian, A.: On the relationship between cloud water composition and cloud droplet number concentration, Atmos. Chem. Phys., 20, 7645-7665, 10.5194/acp-20-7645-2020, 2020.

Mardi, A. H., Dadashazar, H., MacDonald, A. B., Crosbie, E., Coggon, M. M., Aghdam, M. A., Woods, R. K., Jonsson, H. H., Flagan, R. C., Seinfeld, J. H., and Sorooshian, A.: Effects of biomass burning on stratocumulus droplet characteristics, drizzle rate, and composition, J. Geophys. Res. Atmos., 124, 12301-12318, 10.1029/2019JD031159, 2019.

Marinoni, A., Laj, P., Sellegri, K., and Mailhot, G.: Cloud chemistry at the Puy de Dôme: variability and relationships with environmental factors, Atmos. Chem. Phys., 4, 715-728, 10.5194/acp-4-715-2004, 2004.

McNaughton, C. S., Clarke, A. D., Howell, S. G., Pinkerton, M., Anderson, B., Thornhill, L., Hudgins, C., Winstead, E., Dibb, J. E., Scheuer, E., and Maring, H.: Results from the DC-8 Inlet Characterization Experiment (DICE): Airborne versus surface sampling of mineral dust and sea salt aerosols, Aerosol Sci. Tech., 41, 136-159, 10.1080/02786820601118406, 2007.

Mochida, M., Umemoto, N., Kawamura, K., and Uematsu, M.: Bimodal size distribution of C2-C4 dicarboxylic acids in the marine aerosols, Geophys. Res. Lett., 30, 1672, 10.1029/2003gl017451, 2003.

Mochizuki, T., Kawamura, K., Yamaguchi, T., and Noguchi, I.: Distributions and sources of water-soluble organic acids in fog water from mountain site (Lake Mashu) of Hokkaido, Japan, Geochem. J., 54, 315-326, 10.2343/geochemj.2.0601, 2020.

Narukawa, M., Kawamura, K., Takeuchi, N., and Nakajima, T.: Distribution of dicarboxylic acids and carbon isotopic compositions in aerosols from 1997 Indonesian forest fires, Geophys. Res. Lett., 26, 3101-3104, 10.1029/1999gl010810, 1999.

965 Page, S. E., Siegert, F., Rieley, J. O., Boehm, H.-D. V., Jaya, A., and Limin, S.: The amount of
966 carbon released from peat and forest fires in Indonesia during 1997, Nature, 420, 61-65,
967 10.1038/nature01131, 2002.

968 Pringle, K., Tost, H., Pozzer, A., Pöschl, U., and Lelieveld, J.: Global distribution of the effective
969 aerosol hygroscopicity parameter for CCN activation, Atmos. Chem. Phys., 10, 5241-5255,
970 10.5194/acp-10-5241-2010, 2010.

971 PSA: Highlights of the Philippine population 2015 census of population:
972 https://psa.gov.ph/content/highlights-philippine-population-2015-census-population, access:
973 January 7, 2016.

974 Raja, S., Raghunathan, R., Yu, X.-Y., Lee, T., Chen, J., Kommalapati, R. R., Murugesan, K.,
975 Shen, X., Qingzhong, Y., Valsaraj, K. T., and Collett Jr., J. L.: Fog chemistry in the Texas–
976 Louisiana gulf coast corridor, Atmos. Environ., 42, 2048-2061, 10.1016/j.atmosenv.2007.12.004,
977 2008.

978 Raja, S., Raghunathan, R., Kommalapati, R. R., Shen, X., Collett Jr., J. L., and Valsaraj, K. T.:
979 Organic composition of fogwater in the Texas–Louisiana gulf coast corridor, Atmos. Environ.,
980 43, 4214-4222, 10.1016/j.atmosenv.2009.05.029, 2009.

981 Reid, J. S., Hobbs, P. V., Ferek, R. J., Blake, D. R., Martins, J. V., Dunlap, M. R., and Liousse,
982 C.: Physical, chemical, and optical properties of regional hazes dominated by smoke in Brazil, J.
983 Geophys. Res. Atmos., 103, 32059-32080, 10.1029/98jd00458, 1998.

984 Reid, J. S., Hyer, E. J., Johnson, R. S., Holben, B. N., Yokelson, R. J., Zhang, J., Campbell, J. R.,
985 Christopher, S. A., Di Girolamo, L., Giglio, L., Holz, R. E., Kearney, C., Miettinen, J., Reid, E.
986 A., Turk, F. J., Wang, J., Xian, P., Zhao, G., Balasubramanian, R., Chew, B. N., Janjai, S.,
987 Lagrosas, N., Lestari, P., Lin, N.-H., Mahmud, M., Nguyen, A. X., Norris, B., Oanh, N. T. K.,
988 Oo, M., Salinas, S. V., Welton, E. J., and Liew, S. C.: Observing and understanding the
989 Southeast Asian aerosol system by remote sensing: An initial review and analysis for the Seven
990 Southeast Asian Studies (7SEAS) program, Atmos. Res., 122, 403-468,
991 10.1016/j.atmosres.2012.06.005, 2013.

992 Reid, J. S., Lagrosas, N. D., Jonsson, H. H., Reid, E. A., Sessions, W. R., Simpas, J. B., Uy, S.
993 N., Boyd, T., Atwood, S. A., Blake, D. R., Campbell, J. R., Cliff, S. S., Holben, B. N., Holz, R.
994 E., Hyer, E. J., Lynch, P., Meinardi, S., Posselt, D. J., Richardson, K. A., Salinas, S. V., Smirnov,
995 A., Wang, Q., Yu, L., and Zhang, J.: Observations of the temporal variability in aerosol
996 properties and their relationships to meteorology in the summer monsoonal South China Sea/East
997 Sea: the scale-dependent role of monsoonal flows, the Madden–Julian Oscillation, tropical
998 cyclones, squall lines and cold pools, Atmos. Chem. Phys., 15, 1745-1768, 10.5194/acp-15-
999 1745-2015, 2015.

1000 Reid, J. S., Xian, P., Holben, B. N., Hyer, E. J., Reid, E. A., Salinas, S. V., Zhang, J., Campbell,
1001 J. R., Chew, B. N., Holz, R. E., Kuciauskas, A. P., Lagrosas, N., Posselt, D. J., Sampson, C. R.,
1002 Walker, A. L., Welton, E. J., and Zhang, C.: Aerosol meteorology of the Maritime Continent for
1003 the 2012 7SEAS southwest monsoon intensive study – Part 1: regional-scale phenomena, Atmos.
1004 Chem. Phys., 16, 14041-14056, 10.5194/acp-16-14041-2016, 2016.

1005 Reyes-Rodríguez, G. J., Gioda, A., Mayol-Bracero, O. L., and Collett Jr., J.: Organic carbon,
1006 total nitrogen, and water-soluble ions in clouds from a tropical montane cloud forest in Puerto
1007 Rico, Atmos. Environ., 43, 4171-4177, 10.1016/j.atmosenv.2009.05.049, 2009.

1008 Rinaldi, M., Decesari, S., Carbone, C., Finessi, E., Fuzzi, S., Ceburnis, D., O'Dowd, C. D.,
1009 Sciare, J., Burrows, J. P., Vrekoussis, M., Ervens, B., Tsigaridis, K., and Facchini, M. C.:
1010 Evidence of a natural marine source of oxalic acid and a possible link to glyoxal, J. Geophys.
1011 Res. Atmos., 116, D16204, 10.1029/2011JD015659, 2011.

1012 Rogge, W. F., Mazurek, M. A., Hildemann, L. M., Cass, G. R., and Simoneit, B. R. T.:
1013 Quantification of urban organic aerosols at a molecular level: Identification, abundance and
1014 seasonal variation, Atmos. Environ. A-Gen., 27, 1309-1330, 10.1016/0960-1686(93)90257-y,
1015 1993.

1016 Rolph, G., Stein, A., and Stunder, B.: Real-time Environmental Applications and Display
1017 sYstem: READY, Environ. Modell. Softw., 95, 210-228, 10.1016/j.envsoft.2017.06.025, 2017.

1018 Saltzman, E. S., Savoie, D. L., Zika, R. G., and Prospero, J. M.: Methane sulfonic acid in the
1019 marine atmosphere, J. Geophys. Res. Oceans, 88, 10897-10902, 10.1029/JC088iC15p10897,
1020 1983.

1021 Seinfeld, J. H., and Pandis, S. N.: Atmospheric Chemistry and Physics, 3rd ed., Wiley-
1022 Interscience, New York, NY, 2016.

1023 Shen, X.: Aqueous Phase Sulfate Production in Clouds at Mt. Tai in Eastern China, Ph.D.,
1024 Atmospheric Science, Colorado State University, Fort Collins, 193 pp., 2011.

1025 Shingler, T., Dey, S., Sorooshian, A., Brechtel, F., Wang, Z., Metcalf, A., Coggon, M.,
1026 Muehnenstaedt, J., Russell, L., Jonsson, H., and Seinfeld, J. H.: Characterisation and airborne
1027 deployment of a new counterflow virtual impactor inlet, Atmos. Meas. Tech., 5, 1259-1269,
1028 10.5194/amt-5-1259-2012, 2012.

1029 Sorooshian, A., Varutbangkul, V., Brechtel, F. J., Ervens, B., Feingold, G., Bahreini, R.,
1030 Murphy, S. M., Holloway, J. S., Atlas, E. L., Buzorius, G., Jonsson, H., Flagan, R. C., and
1031 Seinfeld, J. H.: Oxalic acid in clear and cloudy atmospheres: Analysis of data from International
1032 Consortium for Atmospheric Research on Transport and Transformation 2004, J. Geophys. Res.
1033 Atmos., 111, D23S45, 10.1029/2005jd006880, 2006.

1034 Sorooshian, A., Crosbie, E., Maudlin, L. C., Youn, J. S., Wang, Z., Shingler, T., Ortega, A. M.,
1035 Hersey, S., and Woods, R. K.: Surface and airborne measurements of organosulfur and
1036 methanesulfonate over the Western United States and coastal areas, J. Geophys. Res. Atmos.,
1037 120, 8535-8548, 10.1002/2015JD023822, 2015.

1038 Stahl, C., Cruz, M. T., Bañaga, P. A., Betito, G., Braun, R. A., Aghdam, M. A., Cambaliza, M.
1039 O., Lorenzo, G. R., MacDonald, A. B., Hilario, M. R. A., Pabroa, P. C., Yee, J. R., Simpas, J. B.,
1040 and Sorooshian, A.: Sources and characteristics of size-resolved particulate organic acids and
1041 methanesulfonate in a coastal megacity: Manila, Philippines, Atmos. Chem. Phys., 20, 15907-
1042 15935, 10.5194/acp-20-15907-2020, 2020.

1043 Stefan, M. I., Hoy, A. R., and Bolton, J. R.: Kinetics and mechanism of the degradation and
1044 mineralization of acetone in dilute aqueous solution sensitized by the UV photolysis of hydrogen
1045 peroxide, Environ. Sci. Technol., 30, 2382-2390, 10.1021/es950866i, 1996.

1046 Stein, A. F., Draxler, R. R., Rolph, G. D., Stunder, B. J. B., Cohen, M. D., and Ngan, F.:
1047 NOAA's HYSPLIT Atmospheric Transport and Dispersion Modeling System, B. Am. Meteorol.
1048 Soc., 96, 2059-2077, 10.1175/bams-d-14-00110.1, 2015.

1049 Stockwell, C. E., Jayarathne, T., Cochrane, M. A., Ryan, K. C., Putra, E. I., Saharjo, B. H.,
1050 Nurhayati, A. D., Albar, I., Blake, D. R., Simpson, I. J., Stone, E. A., and Yokelson, R. J.: Field
1051 measurements of trace gases and aerosols emitted by peat fires in Central Kalimantan, Indonesia,
1052 during the 2015 El Niño, Atmos. Chem. Phys., 16, 11711-11732, 10.5194/acp-16-11711-2016,
1053 2016.

1054 Straub, D. J., Lee, T., and Collett Jr., J. L.: Chemical composition of marine stratocumulus
1055 clouds over the eastern Pacific Ocean, J. Geophys. Res. Atmos., 112, D04307,
1056 10.1029/2006JD007439, 2007.

1057 Straub, D. J., Hutchings, J. W., and Herckes, P.: Measurements of fog composition at a rural site,
1058 Atmos. Environ., 47, 195-205, 10.1016/j.atmosenv.2011.11.014, 2012.

1059 Straub, D. J.: Radiation fog chemical composition and its temporal trend over an eight year
1060 period, Atmos. Environ., 148, 49-61, 10.1016/j.atmosenv.2016.10.031, 2017.

1061 Sullivan, R. C., and Prather, K. A.: Investigations of the diurnal cycle and mixing state of oxalic
1062 acid in individual particles in Asian aerosol outflow, Environ. Sci. Technol., 41, 8062-8069,
1063 10.1021/es071134g, 2007.

1064 Talbot, R., Beecher, K., Harriss, R., and Cofer III, W.: Atmospheric geochemistry of formic and
1065 acetic acids at a mid-latitude temperate site, J. Geophys. Res. Atmos., 93, 1638-1652,
1066 10.1029/JD093iD02p01638, 1988.

1067 Tan, Y., Carlton, A. G., Seitzinger, S. P., and Turpin, B. J.: SOA from methylglyoxal in clouds
1068 and wet aerosols: Measurement and prediction of key products, Atmos. Environ., 44, 5218-5226,
1069 10.1016/j.atmosenv.2010.08.045, 2010.

1070 Thomas, D. A., Coggon, M. M., Lignell, H., Schilling, K. A., Zhang, X., Schwantes, R. H.,
1071 Flagan, R. C., Seinfeld, J. H., and Beauchamp, J. L.: Real-time studies of iron oxalate-mediated
1072 oxidation of glycolaldehyde as a model for photochemical aging of aqueous tropospheric
1073 aerosols, Environ. Sci. Technol., 50, 12241-12249, 10.1021/acs.est.6b03588, 2016.

1074 Tsai, Y. I., Sopajaree, K., Chotruksa, A., Wu, H.-C., and Kuo, S.-C.: Source indicators of
1075 biomass burning associated with inorganic salts and carboxylates in dry season ambient aerosol
1076 in Chiang Mai Basin, Thailand, Atmos. Environ., 78, 93-104, 10.1016/j.atmosenv.2012.09.040,
1077 2013.

1078 Turekian, V. C., Macko, S. A., and Keene, W. C.: Concentrations, isotopic compositions, and
1079 sources of size-resolved, particulate organic carbon and oxalate in near-surface marine air at
1080 Bermuda during spring, J. Geophys. Res. Atmos., 108, 4157, 10.1029/2002JD002053, 2003.

1081 Turpin, B. J., and Lim, H.-J.: Species contributions to PM2.5 mass concentrations: Revisiting
1082 common assumptions for estimating organic mass, Aerosol Sci. Tech., 35, 602-610,
1083 10.1080/02786820119445, 2001.

1084 Wang, J., Ge, C., Yang, Z., Hyer, E. J., Reid, J. S., Chew, B.-N., Mahmud, M., Zhang, Y., and
1085 Zhang, M.: Mesoscale modeling of smoke transport over the Southeast Asian Maritime
1086 Continent: Interplay of sea breeze, trade wind, typhoon, and topography, Atmos. Res., 122, 486-
1087 503, 10.1016/j.atmosres.2012.05.009, 2013.

1088 Wang, Y., Zhuang, G., Chen, S., An, Z., and Zheng, A.: Characteristics and sources of formic,
1089 acetic and oxalic acids in PM2.5 and PM10 aerosols in Beijing, China, Atmos. Res., 84, 169-
1090 181, 10.1016/j.atmosres.2006.07.001, 2007.

1091 Wang, Y., Guo, J., Wang, T., Ding, A., Gao, J., Zhou, Y., Collett Jr., J. L., and Wang, W.:
1092 Influence of regional pollution and sandstorms on the chemical composition of cloud/fog at the
1093 summit of Mt. Taishan in northern China, Atmos. Res., 99, 434-442,
1094 10.1016/j.atmosres.2010.11.010, 2011.

1095 Xian, P., Reid, J. S., Atwood, S. A., Johnson, R. S., Hyer, E. J., Westphal, D. L., and Sessions,
1096 W.: Smoke aerosol transport patterns over the Maritime Continent, Atmos. Res., 122, 469-485,
1097 10.1016/j.atmosres.2012.05.006, 2013.

1098 Yang, F., Gu, Z., Feng, J., Liu, X., and Yao, X.: Biogenic and anthropogenic sources of oxalate
1099 in PM2.5 in a mega city, Shanghai, Atmos. Res., 138, 356-363, 10.1016/j.atmosres.2013.12.006,
1100 2014.

1101 Yao, L., Yang, L., Chen, J., Wang, X., Xue, L., Li, W., Sui, X., Wen, L., Chi, J., and Zhu, Y.:
1102 Characteristics of carbonaceous aerosols: Impact of biomass burning and secondary formation in
1103 summertime in a rural area of the North China Plain, Sci. Total Environ., 557-558, 520-530,
1104 10.1016/j.scitotenv.2016.03.111, 2016.

1105 Youn, J.-S., Crosbie, E., Maudlin, L., Wang, Z., and Sorooshian, A.: Dimethylamine as a major
1106 alkyl amine species in particles and cloud water: Observations in semi-arid and coastal regions,
1107 Atmos. Environ., 122, 250-258, 10.1016/j.atmosenv.2015.09.061, 2015.

1108 Yuan, H., Wang, Y., and Zhuang, G.: MSA in Beijing aerosol, Chinese Sci. Bull., 49, 1020-
1109 1025, 10.1007/bf03184031, 2004.

1110 Zhang, Q., and Anastasio, C.: Chemistry of fog waters in California's Central Valley—Part 3:
1111 concentrations and speciation of organic and inorganic nitrogen, Atmos. Environ., 35, 5629-
1112 5643, 10.1016/S1352-2310(01)00337-5, 2001.

1113   Zhang, Q., Worsnop, D., Canagaratna, M., and Jimenez, J.: Hydrocarbon-like and oxygenated
1114   organic aerosols in Pittsburgh: insights into sources and processes of organic aerosols, Atmos.
1115   Chem. Phys., 5, 3289-3311, 10.5194/acp-5-3289-2005, 2005.

1116   Ziemba, L. D., Griffin, R. J., Whitlow, S., and Talbot, R. W.: Characterization of water-soluble
1117   organic aerosol in coastal New England: Implications of variations in size distribution, Atmos.
1118   Environ., 45, 7319-7329, 10.1016/j.atmosenv.2011.08.022, 2011.

1119

1120

1121 **Table 1:** Mass concentration limits of detection (LOD), minimum, maximum, mean, one
1122 standard deviation, and median values (ppb; left), in addition to mass fraction (%; right) for the
1123 159 CAMP^{2}Ex cloud water samples with TOC data; note that mass fraction values depend on the
1124 C mass of each organic species shown. Total measured mass is defined as the sum of TOM, Na^+,
1125 NH_4^+, K^+, Mg^{2+}, Ca^{2+}, Cl^-, NO_2^-, Br^-, NO_3^-, and SO_4^{2-}. MCA – monocarboxylic acids, DCA –
1126 dicarboxylic acids, MSA – methanesulfonate, DMA – dimethylamine, MO – measured organics,
1127 TOM – total organic matter, DL – detection limit.

	LOD	Concentration (ppb)					Mass Fraction (%)				
		Min	Max	Median	Mean	Stdev	Min	Max	Median	Mean	Stdev
Glycolate	98.76	<DL	224.8	10.65	13.49	20.34	0.0	35.0	0.6	1.3	3.7
Acetate	6.376	<DL	3926	159.4	251.4	409.9	0.0	100.0	10.5	14.7	20.5
Formate	19.77	2.095	3819	66.58	188.5	432.5	0.2	100.0	3.8	5.4	9.3
Pyruvate	5.452	<DL	296.9	5.359	24.35	41.28	0.0	56.1	0.5	1.3	4.5
MCA	-	13.40	8042	253.4	477.8	857.8	0.6	100.0	16.9	22.6	33.9
Glutarate	43.70	<DL	258.7	<DL	6.824	27.32	0.0	1.0	0.0	0.1	0.2
Adipate	39.21	<DL	71.45	2.977	5.331	8.306	0.0	43.7	0.4	1.0	3.6
Succinate	38.64	<DL	1372	<DL	55.23	137.7	0.0	9.3	0.0	1.6	2.4
Maleate	14.81	<DL	14.73	<DL	0.6880	2.310	0.0	0.8	0.0	0.0	0.1
Oxalate	55.23	<DL	1135	38.64	95.65	148.2	0.0	43.9	1.7	2.8	4.3
DCA	-	1.479	2766	61.40	163.7	295.3	0.1	69.8	3.3	5.5	7.5
MSA	88.01	<DL	24.79	3.9	5.107	5.313	0.0	0.9	0.1	0.1	0.1
DMA	56.97	<DL	183.8	<DL	11.16	32.41	0.0	45.3	0.0	1.7	6.3
MO	-	29.46	10820	334.3	657.7	1125	1.5	100.0	23.8	30.0	41.2
TOC	0.05	18.00	13660	546	902	1435	↑ *Relative to TOC (%)* ↑				
Inorg/TOM	-	0.05	90.29	3.31	5.82	8.56	Relative to total measured				
pH	-	3.79	5.93	5.19	5.04	0.51	↓ concentrations (%) ↓				
MO	-	-	-	-	-	-	0.8	57.6	7.2	10.3	9.2
TOM	-	32.40	24590	983	1624	2584	1.1	95.1	23.2	30.7	24.5
Inorganic	-	25.99	117900	3894	8651	13645	4.9	98.9	76.8	69.3	24.5
Na	16.62	<DL	29280	609	1650	3192	0.0	26.6	9.5	10.0	7.8
NH$_4$	176.8	<DL	8099	427	804	1010	0.0	68.1	7.2	11.2	13.2
K	142.4	<DL	1211	21.40	75.35	144	0.0	21.8	0.5	0.8	2.0
Mg	46.20	<DL	3701	57.87	182	379	0.0	4.0	1.0	1.1	0.9
Ca	74.81	<DL	1951	118	201	277	0.0	25.2	1.6	3.5	4.6
Cl	76.59	<DL	38200	908	2451	4438	0.0	42.7	15.3	16.0	11.7
NO$_2$	46.24	<DL	16.31	<DL	1.551	3.304	0.0	0.4	0.0	0.0	0.1
Br	7.817	<DL	44.05	1.398	4.081	7.120	0.0	0.2	0.0	0.0	0.0
NO$_3$	17.33	<DL	26560	572	1488	2925	0.0	43.4	10.4	12.6	8.2
SO$_4$	414.7	2.318	15680	868	1795	2495	0.4	34.9	14.1	14.0	8.5

1128

1129

Table 2: Speciated concentrations of organics (ppb) for each case study, where the first group of rows are monocarboxylic acids (MCA), the second group of rows are dicarboxylic acids (DCA), the third group of rows are other organics plus total measured organics (MO) and total organic carbon (TOC), inorganic ions, and the fifth group are select ratios. n = number of samples.

	North (n = 20)					East (n = 11)					Biomass Burning (n = 4)					Clark (n = 25)				
	Min	Max	Median	Mean	Stdev	Min	Max	Median	Mean	Stdev	Min	Max	Median	Mean	Stdev	Min	Max	Median	Mean	Stdev
Glycolate	5.963	37.18	15.80	17.59	9.15	5.339	30.00	12.21	13.68	7.249	<DL	46.86	7.20	15.31	22.10	<DL	53.42	6.900	11.68	14.61
Acetate	1.935	288.8	184.9	177.8	72.96	301.7	423.5	358.6	359.0	40.71	47.85	3926	1704	1845	1668	<DL	1105	185.2	296.7	325.8
Formate	10.28	232.2	62.66	83.16	79.65	61.02	492.8	248.3	258.2	122.2	151.0	3819	2370	2178	1589	2.422	1041	152.0	266.1	316.8
Pyruvate	2.143	126.5	35.91	42.98	38.98	7.502	78.24	24.65	32.25	21.01	<DL	296.9	103.4	125.9	126.1	1.072	161.8	16.08	30.31	35.84
MCA	25.32	632.2	299.9	321.5	183.6	431.3	923.7	673.2	663.2	142.7	245.7	8042	4184	4164	3336	31.93	2066	369.2	604.7	641.9
Glutarate	<DL	10.18	<DL	1.527	2.758	<DL	10.86	4.074	5.122	3.672	62.46	258.7	140.2	150.4	82.20	<DL	62.46	1.358	9.423	16.85
Adipate	<DL	17.44	<DL	5.146	6.266	<DL	<DL	<DL	<DL	<DL	<DL	<DL	<DL	<DL	<DL	<DL	37.43	<DL	3.777	7.888
Succinate	<DL	136.2	28.09	42.30	47.84	15.45	176.9	63.90	74.11	57.27	24.58	1372	416	557.0	575.6	<DL	498.5	18.96	67.74	123.7
Maleate	<DL	<DL	<DL	<DL	<DL	<DL	<DL	<DL	<DL	<DL	<DL	11.61	5.360	5.583	6.456	<DL	14.73	<DL	2.714	4.170
Oxalate	37.53	330.4	124.8	148.7	81.47	52.51	311.2	123.3	153.6	81.06	303.8	1135	520.1	619.7	360.1	5.547	448.9	43.63	88.33	103.9
DCA	67.84	467.1	149.3	197.6	125.2	80.60	493.4	194.1	232.9	136.4	735.8	2766	914.6	1333	968.9	7.673	1010	72.10	172.0	238.0
MSA	1.550	14.72	7.748	8.290	3.160	3.10	17.82	10.07	10.57	4.400	<DL	24.79	3.874	8.135	11.69	<DL	10.85	3.874	4.184	3.620
DMA	<DL	<DL	<DL	<DL	<DL	<DL	<DL	<DL	<DL	<DL	<DL	<DL	<DL	<DL	<DL	<DL	61.25	<DL	6.454	15.89
MO	99.36	1089	483.8	527.5	301.6	567.0	1364	855.6	906.6	269.4	1017	10820	5094	5505	4187	54.05	3054	433	787.3	837.3
TOC	364.0	1085	555.0	636.1	230.4	663.0	1570	985.0	1051	330.6	4974	13660	7366	8342	3730	220.0	3362	849	1181	920.2
Na^+	693.2	11870	2273	3238	2861	617.7	6546	1970	2569	1738	832.6	4425	2160	2394	1624	12.28	5870	624.9	1105	1403
NH_4^+	180.6	1955	644.4	847.0	515.5	512.7	2379	1307	1432	587.4	2517	8099	3685	4496	2483	45.29	2880	946.8	1009	814.6
K^+	13.83	404.9	49.69	88.89	99.63	18.32	493.0	66.14	122.9	136.0	132.2	724.3	272.3	350.3	258.4	2.462	264.0	31.82	63.07	75.51
Mg^{2+}	41.42	1338	236.3	347.1	328.3	62.35	668.1	209.4	273.2	182.7	83.62	500.5	242.3	267.2	191.2	<DL	631.2	64.73	117.2	152.6
Ca^{2+}	<DL	764.9	96.85	173.8	218.9	49.47	778.2	166.5	269.2	219.1	105.7	533.5	236.0	277.8	209.7	38.83	903.5	176.8	230.3	183.6
Cl^-	1445	18520	3772	5277	4333	900.2	8357	2760	3510	2196	1126	5989	2553	3055	2124	45.43	9083	990.6	1716	2107
NO_2^-	<DL	<DL	<DL	<DL	<DL	<DL	<DL	<DL	<DL	<DL	<DL	5.598	1.339	2.069	2.670	<DL	16.06	<DL	3.427	5.126
Br^-	3.496	35.66	12.59	15.56	8.036	2.098	6.992	4.195	4.132	1.482	1.398	6.293	2.448	3.147	2.174	<DL	13.29	1.398	2.545	3.204
NO_3^-	477.2	5265	1197	1810	1506	1084	8724	2902	3772	2296	1880	7045	3344	3903	2277	64.84	2759	691.3	930.8	736.1
SO_4^{2-}	1305	12120	3281	4503	2865	1212	5296	2819	3223	1385	2313	9993	4177	5165	3343	23.39	4406	1157	1416	1157
pH	3.92	4.92	4.48	4.40	0.25	4.27	4.92	4.51	4.51	0.20	3.96	4.65	4.35	4.33	0.29	4.66	5.76	5.25	5.29	0.33
Ace/For	0.19	9.66	2.65	4.21	3.26	0.75	5.67	1.52	1.93	1.51	0.32	1.03	0.70	0.69	0.30	0	3.86	0.98	1.12	0.84
Cl^-/Na^+	1.52	2.08	1.69	1.70	0.13	1.28	1.51	1.40	1.40	0.06	1.07	1.43	1.35	1.30	0.16	1.38	3.70	1.69	1.84	0.56
Ca^{2+}/Na^+	0	0.08	0.04	0.04	0.02	0.05	0.14	0.10	0.10	0.03	0.08	0.13	0.12	0.11	0.02	0.05	6.17	0.32	0.99	1.46
K^+/Na^+	0.02	0.03	0.02	0.02	0.01	0.03	0.08	0.04	0.04	0.01	0.10	0.18	0.16	0.15	0.04	0.01	3.93	0.05	0.25	0.78
MO/TOC	0.07	0.37	0.29	0.27	0.08	0.18	0.42	0.29	0.31	0.07	0.04	0.28	0.26	0.21	0.11	0.03	0.57	0.19	0.20	0.13

1130

1131 **Table 3:** Average organic composition for each case study where the first, second, and third
1132 group of rows show percentage contribution (%) of individual components to monocarboxylic
1133 acids (MCA), dicarboxylic acids (DCA), and total organic carbon (TOC), respectively.

Group	Species (%)	North (n = 20)		East (n = 11)		BB (n = 4)		Clark (n = 25)	
		Mean	Stdev	Mean	Stdev	Mean	Stdev	Mean	Stdev
MCA	Glycolate	7.20	9.20	1.84	0.81	5.09	9.87	17.65	29.05
	Acetate	64.03	17.74	64.20	10.85	45.86	14.07	46.35	23.98
	Formate	16.54	9.83	28.62	10.35	46.40	7.24	29.09	11.72
	Pyruvate	12.23	6.90	5.33	2.87	2.65	1.87	6.91	4.90
DCA	Glutarate	0.65	1.00	2.91	1.41	17.15	9.28	4.02	5.02
	Adipate	8.04	9.47	0	0	0	0	16.05	21.48
	Succinate	20.82	20.08	38.52	12.15	41.95	25.27	26.53	25.39
	Maleate	0	0	0	0	0.75	0.88	3.20	5.93
	Oxalate	70.49	12.29	58.57	11.52	40.16	16.50	50.20	17.42
TOC	MSA	0.17	0.05	0.13	0.04	0.01	0.02	0.06	0.07
	DMA	0	0	0	0	0	0	0.43	1.17
	MCA	17.79	6.17	23.66	5.99	16.03	10.13	16.28	11.91
	DCA	8.75	2.65	6.82	2.94	5.21	1.60	3.70	2.67
	MO	26.72	7.86	30.61	7.35	21.25	11.32	20.46	13.34
	Undetected	73.28	7.86	69.39	7.35	78.75	11.32	79.54	13.34

1134
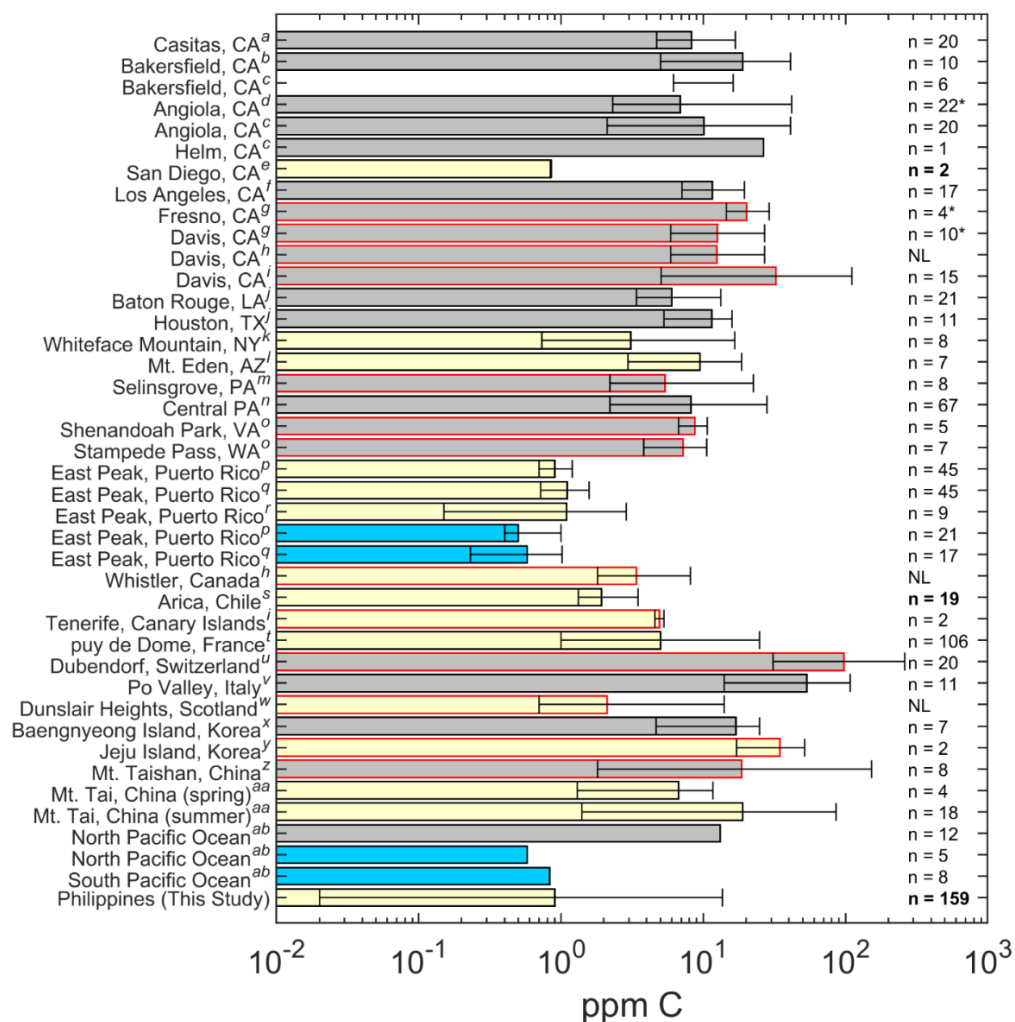
1135

Figure 1: TOC (or DOC if TOC values were unavailable) concentrations reported for past
studies in relation to this work organized by continent. Bars represent the average values and the
error bars represent the minimum and maximum values. The absence of a solid bar means no
average was available. No error bars means there was no range given, and * indicates the median
value was reported rather than an average. Gray, yellow, and blue bars represent studies looking
at fog, clouds, and rain, respectively. Bars that are outlined in black are studies that used TOC
and bars outlined in red are studies that used DOC. The n values represent the number of samples
used in the study and NL means the number of samples were not listed. Bolded n values denote
airborne samples. This figure is similar to that of Figure 2 in Herckes et al. (2013) with
additional information presented and organized by continent. (a - Boris et al. (2018), b - Collett Jr. et
al. (1998), c - Herckes et al. (2002), d - Herckes et al. (2007), e - Straub et al. (2007), f - Erel et al. (1993),
g - Ehrenhauser et al. (2012), h - Ervens et al. (2013), i - Zhang and Anastasio (2001), j - Raja et al.
(2008), k - Cook et al. (2017), l - Hutchings et al. (2008), m - Straub et al. (2012), n - Straub (2017), o -
Anastasio et al. (1994), p - Gioda et al. (2011), q - Gioda et al. (2008), r - Reyes-Rodríguez et al. (2009), s
- Benedict et al. (2012), t - Deguillaume et al. (2014), u - Capel et al. (1990), v - Gelencser et al. (2000),
w - Hadi et al. (1995), x - Boris et al. (2016), y - Decesari et al. (2005), z - Wang et al. (2011), aa - Shen
(2011), ab - Kim et al. (2020))
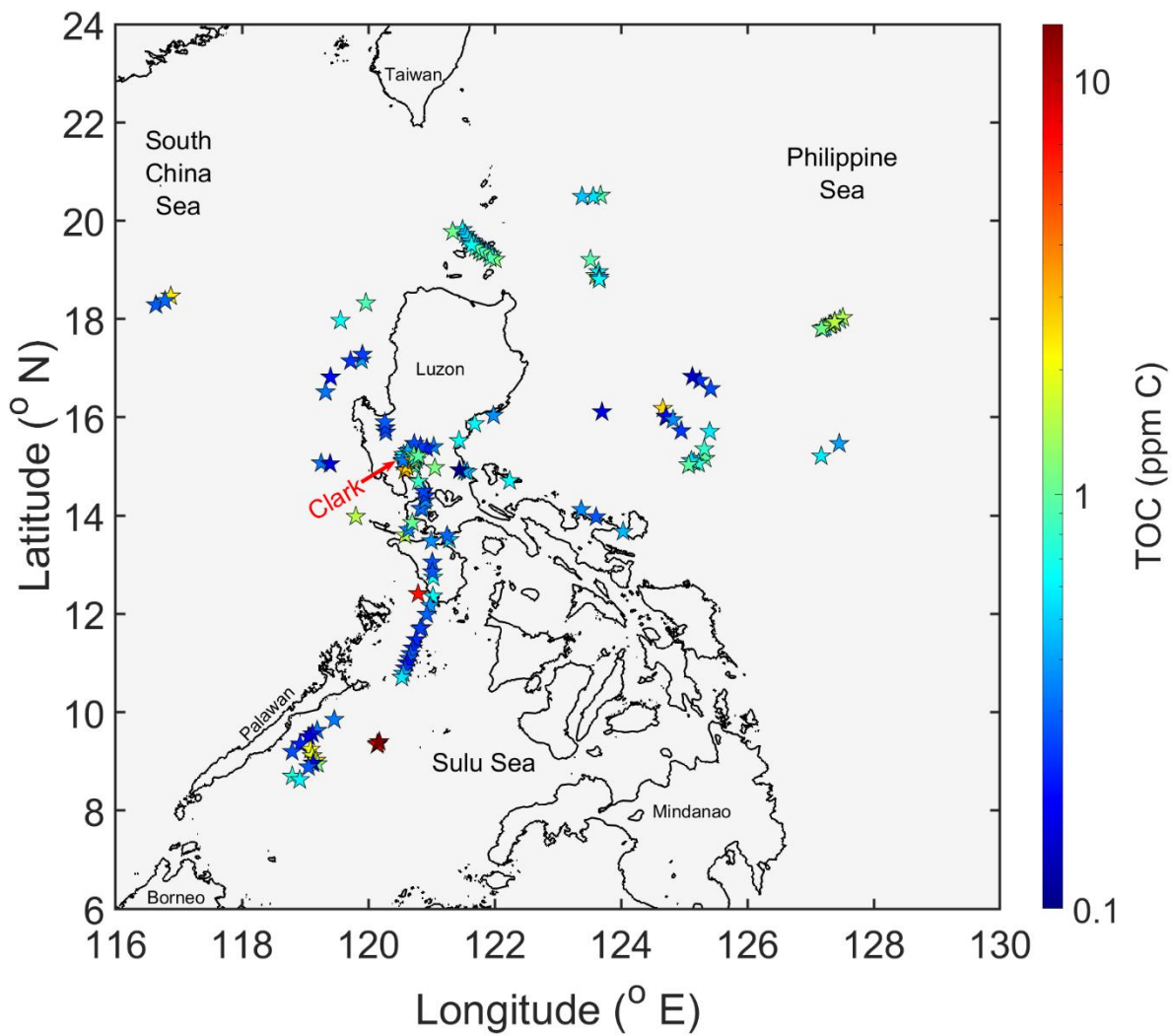
1153

1154 **Figure 2:** Map of sample region where the stars represent the midpoint of the cloud water
1155 samples where total organic carbon (TOC) was measured. Stars are colored by TOC on a
1156 logarithmic scale.

1157
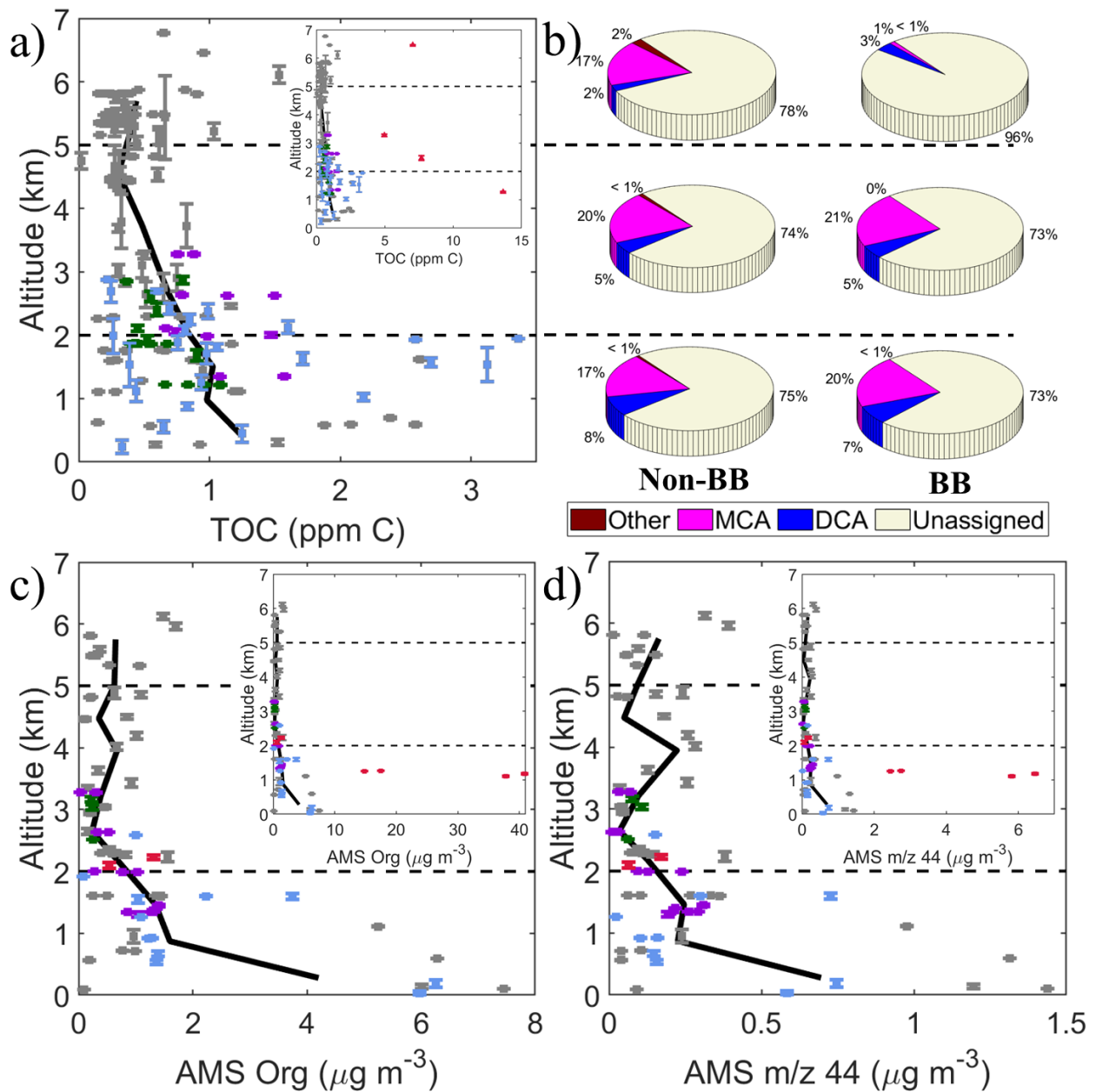
Figure 3. (a) Vertical profile of TOC concentrations (n = 159 samples) with the smaller inset including four samples with enhanced TOC owing to biomass burning (BB) influence. (b) Mass fractions of different subsets of species contributing to TOC at high (> 5 km), mid (2 – 5 km), and low (< 2 km) altitude with the beige area representing undetected species. Vertical profile of AMS (c) organic and (d) m/z 44 corresponding to spatially and temporally adjacent cloud-free periods of the collected cloud water samples. Colors in panels a/b/d represent the case study points in Sect. 4: North (green), East (purple), Biomass Burning (red), Clark (blue), non-case points (gray). The solid black lines in panels a/b/d represent locally-weighted average values. The error bars represent one standard deviation of the altitude variance.
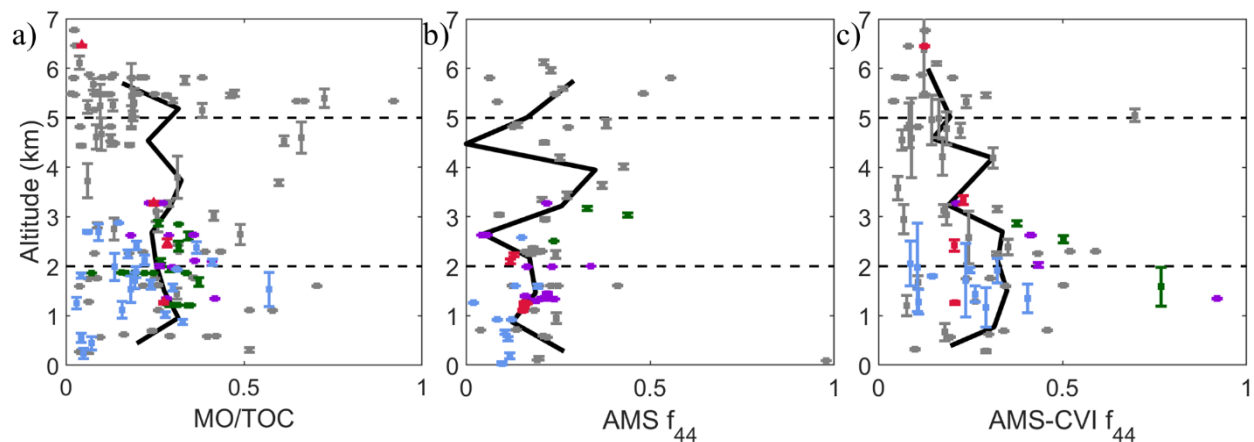
1168

1169 **Figure 4.** Vertical profile of (a) ratio of C mass from measured organics (MO) to TOC for cloud
1170 water samples, (b) AMS f_{44} in cloud-free air, and (c) AMS-CVI f_{44} in cloudy air. AMS data in (b)
1171 corresponds to cloud-free periods that were spatially and temporally adjacent to the collected
1172 cloud water samples, while those in (c) are within the period of cloud water collection times in
1173 cloud. Colors in panels a/b/d represent the same case study points as Figure 3: North (green),
1174 East (purple), Biomass Burning (red), Clark (blue), non-case points (gray). The black lines in
1175 panels a/b/d represent locally-weighted average values.
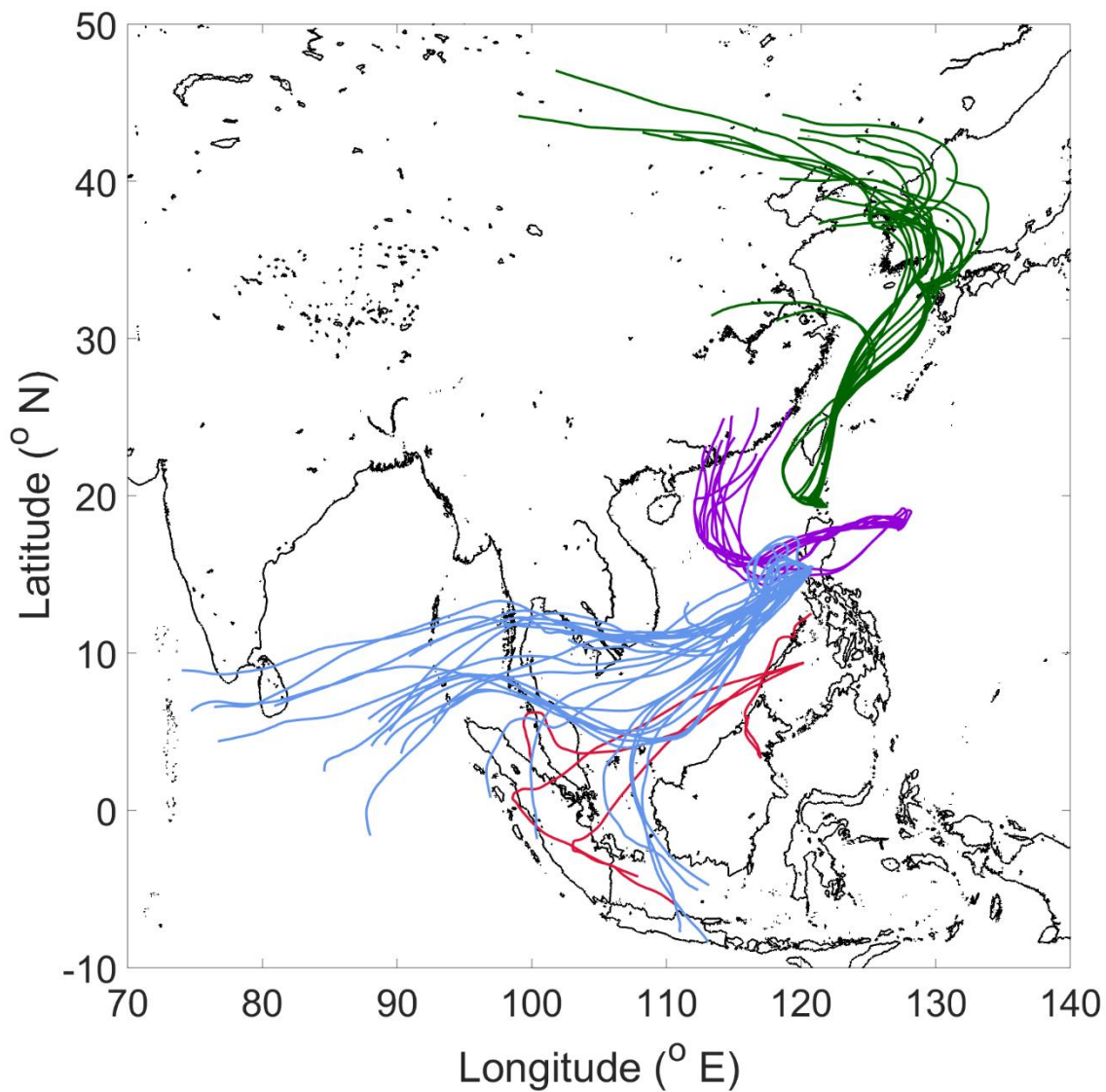
1176

1177 **Figure 5:** Spatial summary of 120-hour back trajectories for each sample included in respective
1178 case study sample sets: North (green; n = 20), East (purple; n = 11), Biomass Burning (red; n =
1179 4), and Clark (blue; n = 25).

1180